Double-target based network in predicting energy consumption in residential buildings

Hossein Moayedi [1,2], Amir Mosavi [3,4],

1 Institute of Research and Development, Duy Tan University, Da Nang, 550000, Viet Nam; hosseinmoayedi@duytan.edu.vn
2 Faculty of Civil Engineering, Duy Tan University, Da Nang 550000, Vietnam.
3 School of Economics and Business, Norwegian University of Life Sciences, 1430 Ås, Norway, **a.mosavi@ieee.org**
4 John von Neumann Faculty of Informatics, Obuda University, 1034 Budapest, Hungary

Abstract: Reliable prediction of sustainable energy consumption is the key to designing environmental friend buildings. In this study, two novel hybrid intelligent methods, namely grasshopper optimization algorithm (GOA), wind-driven optimization (WDO), and biogeography-based optimization (BBO) is employed to optimize the multitarget prediction of heating loads (HLs) and cooling loads (CLs) in heating ventilation and air conditioning (HVAC) systems. Concerning the optimization of applied hybrid algorithms, a series of swarm-based iteration is performed, and the best structure for the abovementioned methods are proposed. Besides, through sensitivity analyzing the relationship between the HLs and CLs and influential factors are highlighted. In other words, the GOA, WDO, and BBO algorithm are mixed with a class of feedforward artificial neural networks (ANN), which called MLP (multi-layer perceptron) to predict the HLs and CLs. According to the provided sensitivity analysis, the WDO with swarm size = 500 proposes the most proper-fitted terms after it has been combined with optimized MLP. The proposed WDO-MLP (training (R^2 correlation=0.977 and RMSE error=0.183) and testing (R^2 correlation=0.973 and RMSE error=0.190)) provided accurate prediction in the heating load and (training (R^2 correlation=0.99 and RMSE error=0.147) and testing (R^2 correlation=0.99 and RMSE error=0.148)) presents the most-fit prediction in the cooling load.

Keywords: Energy efficiency; Heating loads; heating ventilation and air conditioning; metaheuristic; optimization algorithms.

1 Introduction

The concerns about reducing energy consumption in smart cities are growing. Indeed, the rate of energy consumption has risen mainly in the last two decades. For instance, in buildings, an approximate increasing rate of 0.9% per year in the USA as reported by the US EIA [1]. In this regard, the residential buildings (as it is the main concern of the present study) consume 38% of electricity energy approximately. Therefore, almost one-fourth of the world's energy consumed in residential buildings [2]. Considering the climate change,

environmental concerns as well as an overall significant contribution of buildings and their high demands on the consumption of such energy use, new intelligent methods are required to reduce this energy consumption. The rate of energy consumption of buildings has been investigated by various researchers such as Zhou, et al. [3], Ahmad, et al. [4], and Mocanu, et al. [5].

With recent advances in computational intelligence, many scholars have replaced traditional methods with economical and accurate machine learning , deep learning [6-12], decision making [13, 14], and artificial intelligence-based tools [15-19]. These novel approximation techniques are well employed in various engineering field such as in evaluating the environmental concerns [20-30], implications for natural environmental [31-39], water resources management [40-46], energy efficiency [47-55], structural design [56-66], image processing [67-70], feature selection/extraction [71-75], face recognition [76-79], control performance [80], vibration analysis [81], climate change [82], managing the smart cities [83], project management [84], while in the field of medical science artificial intelligence employed to have a better diagnosis of a particular patients [85-89], early diagnosis of them [90, 91], or medical image classification [92]. There have been many novel algorithms enhancing the current predictive neural network-based models. Metaheuristic algorithms have been highly regarded in various problems that demand an optimal solution [90]. The hybrid optimization techniques such as differential evolution [93], data-driven robust optimization [94], whale optimization algorithm [95, 96], harris hawks optimization [93, 97], differential edge detection algorithm [98], many-objective sizing optimization [99], fruit fly optimization [100], moth-flame optimization strategy [101, 102], bacterial foraging optimization [103], ant colony optimization [104], particle swarm optimization (PSO) [105-107], chaos enhanced grey wolf optimization [87], and quantum-enhanced multiobjective large-scale [108].

Zhou, et al. [3] applied a feedforward artificial neural network (ANN) combined with a hybrid system (e.g., considering the multivariable optimization process). The results obtained from their study showed that the generated ANN-based data-driven training algorithm is more reliable than the traditional 'lsqcurvefit' fitting method. Asadi, et al. [109] investigated the energy consumption prediction of the building retrofits. They have used a combination of the ANN and genetic algorithm to find the most proper structure o a hybrid algorithm and to assess the interaction among conflicting objectives. Mocanu, et al. [5] stated that the deep learning-based solution methods are aimed to enhance the estimation level of the predictive network by letting a higher level of abstraction to be implemented. Ahmad, et al. [4] stated that the management of energy-efficient buildings and predicting energy consumption for all buildings are a critical task in decision-makers in order to save effective energy as well as to develop smart cities. They have reviewed some of the employed prediction technique in estimating the building electrical energy using most updated artificial intelligence (AI) based solution. Zhou, et al. [3] investigated on the use of a new hybrid system combined with active cooling, phase change materials, and hybrid ventilations.

Many researchers also have aimed to investigate the links between the HLs and Cls and their most influential parameters such as the speed of the wind, the conditions of the environment climate changing, the rate of light, etc. Budaiwi and Abdou [110] employed successfully the heating, ventilation, and air conditioning (HVAC) system operational

strategies to deduce the amount of consumed energy in buildings. In their study, they used an example of buildings with intermittent occupancy. Nasruddin, et al. [111] studied the HVAC optimization system to measure energy consumption in a particular building dataset. They used ANN as well as multi-objective GA. Their findings provided possible design variables that can help to achieve the best-fit HVAC system. The results proved to be practical in terms of both annual energy consumption and thermal comfort. Min, et al. [112] explored indirect evaporative cooling energy recovery systems (e.g., to pursue a high quality indoor thermal environment) through a new statistical modeling approach. The validation of the proposed model is done using a series of experimental data. Roy, et al. [113] predicted heating load in buildings with employing a hybrid model of (i.e., MARS multivariate adaptive regression splines) and ELM (i.e., extreme learning machine). Liu, et al. [114] studied hierarchical modeling and temperature interval techniques to optimize the prediction of multi-layer hybrid building's cooling and heating load. The obtained results are compared with the basic estimation models, showing that the accuracy of the proposed models is significantly enhanced [114]. Kavaklioglu [115] proposed a new rebuts modeling of cooling and heating loads to have an efficient residential building design. Moayedi, et al. [116] investigated on the social behavior of elephant herds in order to predict cooling load of residential buildings. In this sense, the technique of elephant herding optimization (EHO) is employed to optimize the trend of HVAC system. On the other study, the k-fold cross-validation method was used to validate the proposed hybrid models, as discussed by Qiao, et al. [117]. Conventional modeling such as ordinary least square was employed to have a better comparison between the obtained results and traditional techniques. The results showed that the developed methods are excellent in providing links between the influential factors and the target which were heating and cooling loads.

This study is particularly conducted in the case of residential buildings, where their real operations highly rely on building design criteria. Some of the influential factors that are considered in different previous energy-efficient residential building studies include roof area, relative compactness, overall height, surface area, glazing area, glazing area distribution, wall area, and orientation. The building design codes are trying to reduce the amount of energy consumption by taking two key terms of CLs and HLs. The HVAC is the well-known technology of indoor and vehicular environmental comfort. The concept of HVAC is a key issue in designing the residential building structures such as apartment buildings, hotels, family homes, senior living facilities, office and industrial buildings (e.g., medium to large), hospitals, and skyscrapers. Indeed, the subject of HAVC is not limited to building only, and it can be considered for the commonly used vehicles such as trains, cars, airplanes, large ships as well as submarines which works in the marine environments. The main objective of the HVAC system is to provide acceptable indoor air quality and thermal comfort. Although there is much new technique in the calculation of HLs and CLs, there is still a lack of proper intelligence techniques in the prediction of these parameters. Studying through the current literature, there are numerous studies which have used popular optimization methods such as particle swarm optimization, genetic algorithm, and imperialist competitive algorithm but the lack of multiobjective consideration of both HL and CL as well as more up-to-date hybrid intelligent-based solutions can be a suitable gap of knowledge in the subject of HVAC systems simulation. Therefore, this article recommends several novel multiobjective intelligent based solutions on the herding trend

of grasshopper optimization algorithm (GOA), wind-driven optimization (WDO), and biogeography-based optimization (BBO) to predict the multi targets of HLs and CLs of residential buildings. These algorithms enhance the current drawbacks of ANN-based solutions, such as being trapped in local minima. In this regard, over 33000 model iterations are performed to provide the best-fit structure of combined algorithms. Therefore, the proposed models are enhanced by having a valid sensitivity analysis.

2 Data Provision

The dataset used in this study is initially provided by Tsanas and Xifara [118]. Thereafter employed in other prediction studies such as Guo, et al. [119], Moayedi, et al. [116], Tien Bui, et al. [120], and Gao, et al. [121]. The steps that are taken to fulfill the accuracy requirement of proposed techniques in the current study are illustrated here as well as in Figure 1:

(a) First, data preprocessing: in this step, the collected dataset of heating load and cooling loads are separated randomly into two main sections. This is called the training dataset and testing dataset. As a well-established train/test dataset selection, 70 % of the whole dataset is used to train the models for training a proper predictive network and to make the connection between both targets of HLs and CLs and their influential factors. The rest of the 30% is selected to be the testing and validation datasets. In our example, we selected 30% for the testing dataset only as none of the testing datasets were involved in the learning process.

(b) Second, the programming language of MATLAB 2018 used to (i) defining the most proper structure of the MLP neural network, and (ii) presenting the relevant mathematical outputs of the best MLP structure before sending for GOA, WDO, and BBO algorithms. Thirdly, after a series of trial and error parametric study process (i.e., used to find the most appropriate parameters of the proposed models), the optimization process is performed, and the main multitarget outputs (i.e., in our study was to predict simultaneous prediction of HLs and CLs) are obtained.

In the last step, by employing the remaining 30 % of data (i.e., called testing dataset), the error performance of the proposed models is calculated based on the differences between the real measured valued and the predicted values obtained from the proposed models.

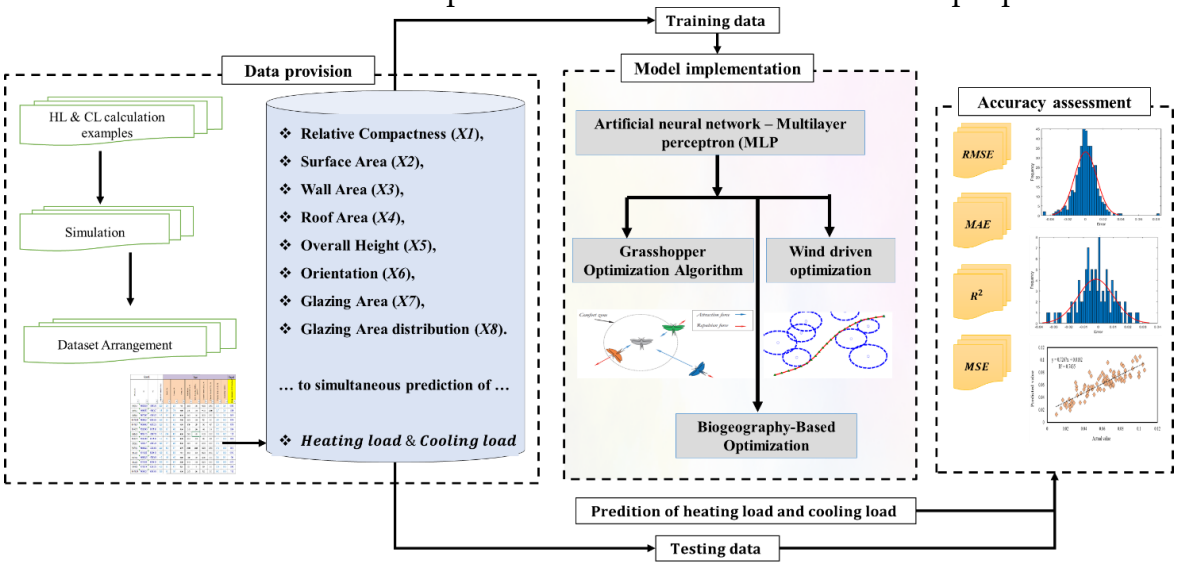

Figure 1: The graphical methodology of this study.

In the following, sections describe the used MLP algorithm, GOA, WDO, and BBO algorithms. The benchmark models of proposed techniques are also presented in section 3.1.2 to 3.1.4.

3 Theoretical background

3.1 Multilayer perceptron

These tools are widely applied for modeling complex engineering issues. Artificial neural networks (ANN), (i.e., also called neural networks) is first introduced by McCulloch and Pitts [122]. It is known as a computing system vaguely inspired by the biological neural networks that idea primary taken from animal brains. This AI based technique will try to make a relationship between a series of input data layers with one or more of output layers by establishing non-linear equations [123]. A common ANN structure includes different elements called input layers, hidden layer(s), and output layer(s) (Figure 2).

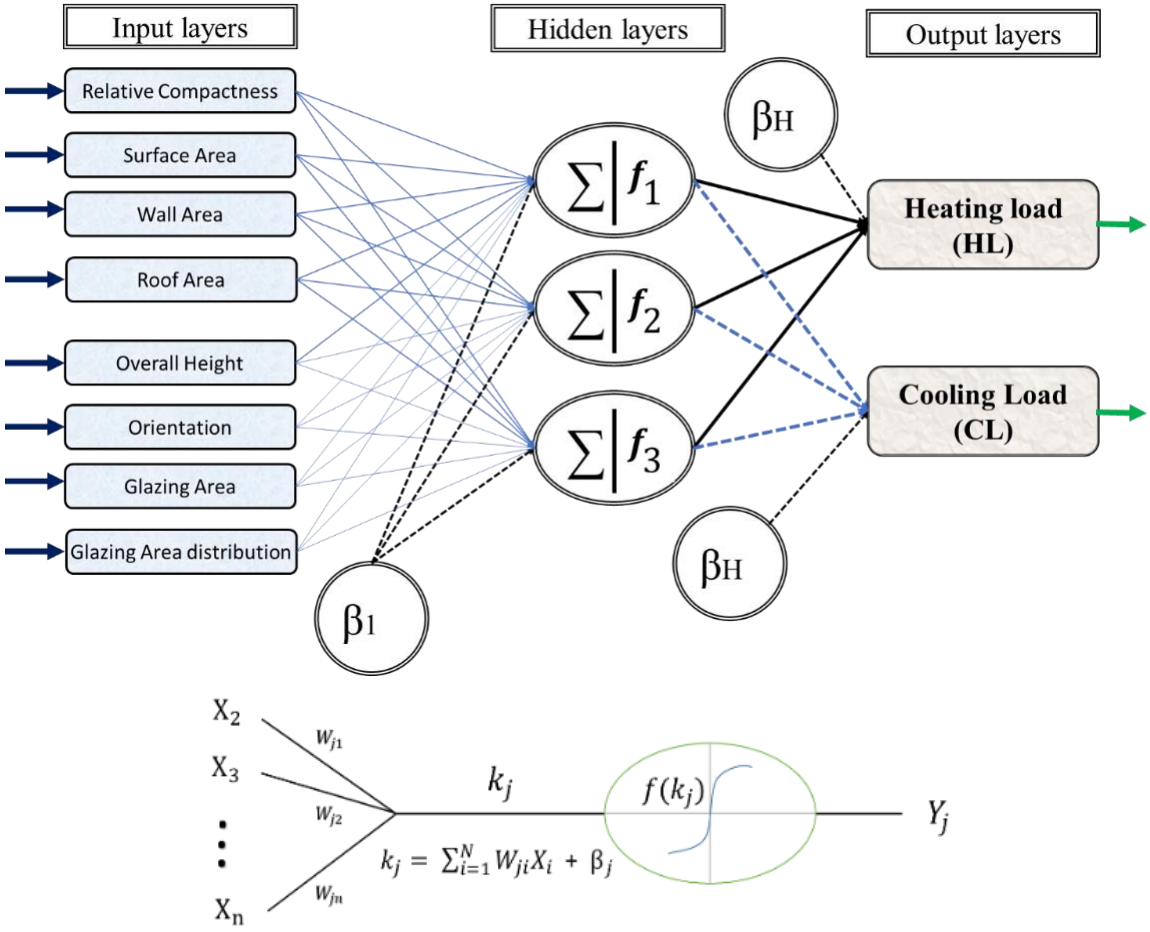

Figure 2: Typical structure and operation of multilayer perceptron

3.2 Grasshopper Optimization Algorithm

Grasshoppers may be seen independently or in a swarm in nature. It is considered as one of the insects feeding on plants. Noting that such insects are considered as a pest (i.e., any plant or animal detrimental) as they mainly harm severely the crops and pasture [124]. The idea of grasshopper optimization algorithm (GOA) is taken from the nature behaviors of

grasshoppers pests, Saremi, et al. [125] developed the GOA for solving searching optimization issues. Like many previously published natural inspired algorithms (e.g., whale optimization algorithm; ant lion optimizer; salp swarm algorithm, etc), the GOA algorithm predicts based on two major steps, first step is exploration where the second step is called exploitation. As is taken from the grasshoppers' behaviors, such steps are performed to seek for a food source. In this first phase (i.e. called the exploitation phase), the agents that are responsible for the search fly locally over the search area. Equation 1 expresses the swarming action of grasshoppers, noting that the term x_i is the position of the ith insect,:

$$h_{w,b}(x) = f^{(n)} \quad (1)$$

$$S_i = \sum_{j=1}^{N} s(d_{ij})\widehat{d_{ij}} \quad (2)$$

$$G_i = -g \times \widehat{e_g} \quad (3)$$

$$A_i = u \times \widehat{e_w} \quad (4)$$

where the initial term of S_i signifies the social relationship, the term G_i represents the gravity force, and the last term of the A_i is the about the importance of wind advection. These parameters are defined in Equations (2), (3), and (4), respectively. Besides, r_1, r_2, and r_3 define some random numbers varying from 0 to 1.

where the strength of social forces is represented by the term s, and d_{ij} Defines the Euclidean distance between the ith and jth grasshoppers. Also, g shows the gravitational constant, $\widehat{e_g}$ Symbolizes a unity vector to the center of the earth. Moreover, u denotes a drift (a constant one), and $\widehat{e_w}$ is a unit vector toward the wind direction. This is worth noting that s in Equation 5 is calculated based on the following relationship, when f and k indicate the attraction severity and attractive length scale, respectively:

$$s(r) = f e^{-r/k} - e^{-r} \quad (5)$$

According to Mafarja, et al. [126], which explored the behavior of the relations for different amounts of the parameters f and k, when the distance between two grasshoppers is in between 0 and 2.079, the repulsion takes place between them. Consequently, if the distance is out of this range (i.e., larger than 2.079), it means that the proposed grasshopper enters a comforting district. This process is illustrated in Figure 3.

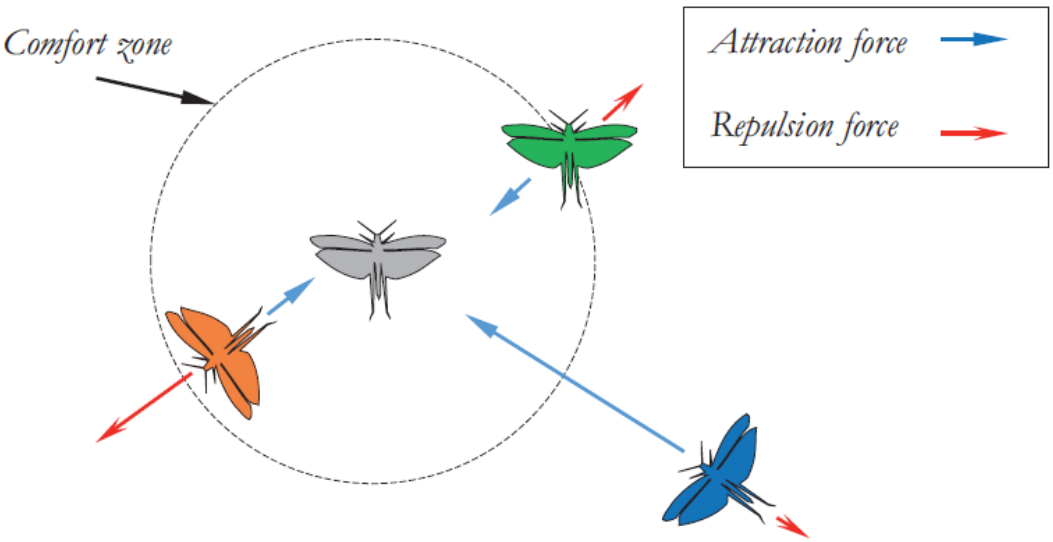

Figure 3: The primitive corrective patterns in the GOA method

3.3 Wind-driven optimization

The technique of wind-driven optimization (WDO) is introduced by Bayraktar, et al. [127]. The early idea of WDO was initially formed for electromagnetics usages. In this sense, four most influential forces for this task are a Coriolis force (F_C), pressure gradient force (F_{PG}), frictional force (F_F) and gravitational force (F_G). The main idea behind the WDO method is that, for reducing the computational complexity, the air parcels are considered weightless and dimensionless. Assuming that δ_V and the ∇P are the finite volume and pressure gradient of the air, and Eq. 6 shows the main force because of the pre-defined pressure gradient. The F_F (as it is shown by Eq. 7) aims to face the air triggered movement by the term F_{PG}. In this regard, the term F_G (i.e., gravitational force illustrated by Eq. 8) pulls the parcels to the earth center from every dimension. Also, the F_C (Eq. 9) attributes to the deflection in the air parcel motions.

$$\overrightarrow{F_{PG}} = -\nabla P \,.\, \delta V \tag{6}$$

$$\overrightarrow{F_F} = -\rho\, \alpha\, \vec{u} \tag{7}$$

$$\overrightarrow{F_G} = \rho \,.\, \delta V . g \tag{8}$$

$$\overrightarrow{F_C} = -2\, \theta \times \vec{u} \tag{9}$$

where in the Eqs 6 to 8, the term $\vec{u}$ is set to be the velocity vector of wind, ρ is the density of a short air parcel, g signifies the gravitational constant, θ symbolizes the earth rotation and finally α is a frictional coefficient.

By considering the above-mentioned influential factors and pre-defined forces along with the ideal gas equation, the finalized equation is provided by Derick, et al. [128]:

$$\overrightarrow{\nabla u} = g + \left(-\nabla P . \frac{RT}{P_{cur}}\right) + (-\alpha\, \vec{u}) + \left(\frac{-2\, \theta \times \vec{u} RT}{P_{cur}}\right) \tag{10}$$

Since the air velocity mainly depends on pressure value the velocity gets adjusted that will brings the higher pressure for the system.
. Therefore, regarding the pressure rank, Eq. 10 is adapted. In this sense, due to the pressure, the known parcels, in a descending sequence, are ranked. Accordingly, the position and velocity are updated by the following equations when i denotes the rank:

$$\overrightarrow{U_{new}} = (1 - \alpha)\,\vec{U}_{cur} - gx_{cur} + \left(\left|1 - \frac{1}{i}\right| .(x_{opt} - x_{cur})RT\right) + \left(\frac{C\ .\ \vec{U}_{otherdirection}}{i}\right) \quad (11)$$

$$\overrightarrow{X_{new}} = \overrightarrow{X_{old}} + \overrightarrow{U_{new}} \quad (12)$$

Where, in the equations 11 and 12, the terms $\vec{U}_{cur}$ and $\overrightarrow{U_{new}}$ signify the velocity value of the current and coming iteration. Noting that the term x is defined as to be the air parcel position. In addition, x_{opt} and x_{cur} are set to be the optimal and current positions. Meanwhile, the other terms such as $\vec{U}_{otherdirection}$ set to be equal $\overrightarrow{F_C}$ while the C is taken to calculated as $C = -2\ RT$. The clarified progressive process updates until one of the stopping criteria met. These criteria can be set objective function or even a pre-defined number of repetitions. Full details of the WDO technique is explained in some previous studies such as Bayraktar, et al. [127] and Bayraktar, et al. [129]

3.4 Biogeography-Based Optimization

Established based on the nature of different species distribution as well as their biogeography knowledge. It is called BBO and first developed by Simon [54]. Later was expanded by other researchers and more particularly by Mirjalili et al. [55], where the initial algorithm was enhanced and combined with MLP structure and become BBO-MLP. Due to its excellent predictivity, many scholars recommended it to be used as in many complex engineering problems. A combination with MLP aimed to optimize the performance of the MLP since the BBO is known as a population search based technique. The flowchart of the original algorithm before to be mixed with MLP is shown in Figure 4. Similar to many other population search-based optimization algorithms, the BBO also gets started by generating a random population called a habitat.

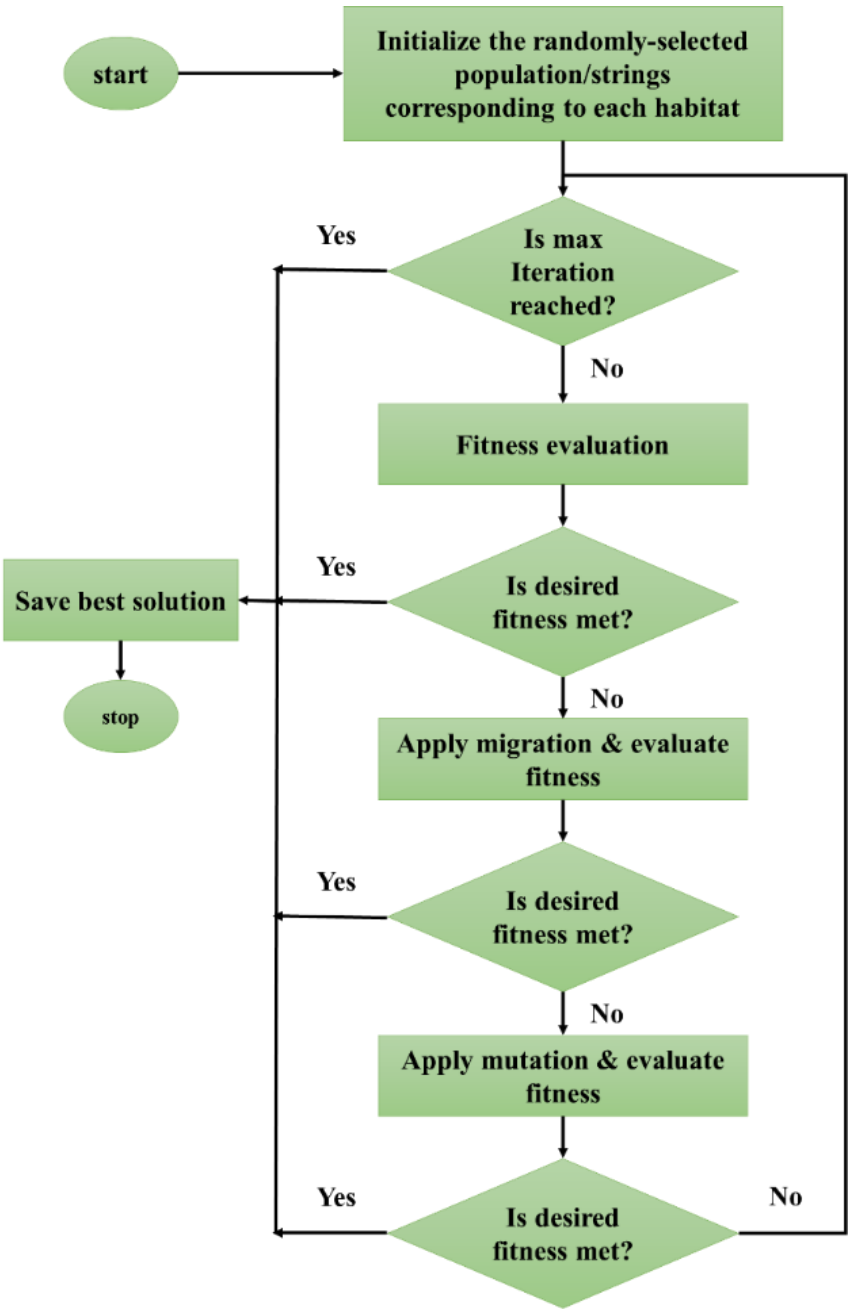

Figure 4. The flowchart of the BBO algorithm.

4 Data collection and statistical analysis

The primary dataset of this study is obtained from Tsanas and Xifara [118] as uploaded in an open-source of machine repository. The dataset prepared according to the Ecotect computer software [130], where 12 different types of residential buildings with changes in their influential design parameters were simulated. The main objective was to measure the values of HL and CL based on the designated residential buildings. Each one of the proposed residential buildings follows the unique structure, such as variation in their design parameters such as relative compactness, roof area, surface area, wall area, orientation, glazing area distribution, overall height, and glazing area. For instance, four orientations, five distribution scenarios, four sets of glazing areas (such as 0, 10, 25 and 40% of the entire floor area), etc. Therefore, a total of 768 design examples were simulated accounting eight key design factors. The targets were both HL and CL that requires for the

particular residential buildings. More description of the employed dataset can be obtained in other related studies such as Chou and Bui [131] and Tsanas and Xifara [118]. In this article, both of the HL, as well as CL, are taken into the calculation procedure as the main target variables. The main aim was that these targets to be predicted by the three proposed hybrid intelligence techniques including GOA-MLP, WDO-MLP, and BBO-MLP. The main dataset includes 768 samples, 537 rows (i.e., 70 %) are chosen for designing the training pattern, and the rest of 231 rows (i.e., 30 %) are taken to assess the validation and to test the trained networks. The scatter plots of Figure 5 show the influential factors that have been used as the main inputs and their relationship with both chosen targets of HL and CL. Spatial distribution of inputs factors versus the HL and CL is also shown in Figure 6. To help to understand the variability of the provided datasets, the descriptive statistics of the input variables are provided and tabulated in Table 1.

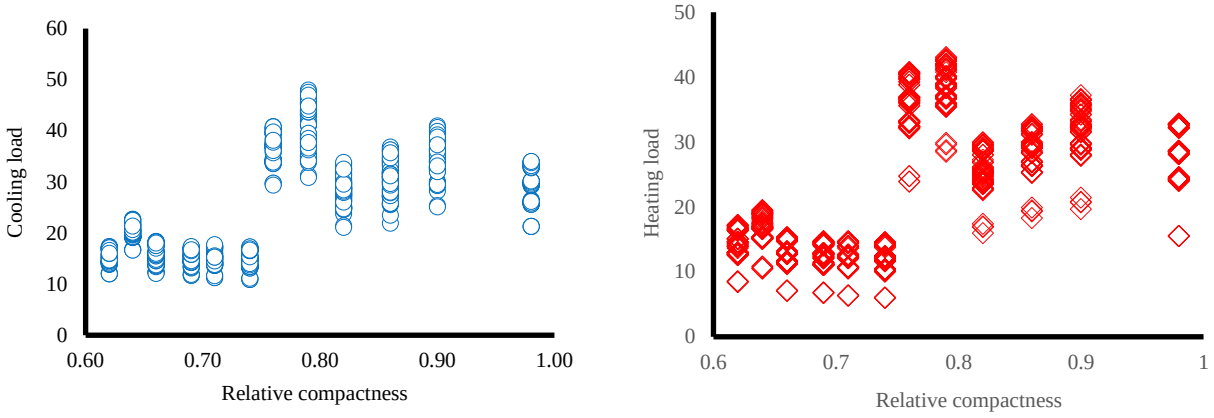

(a) Relative Compactness

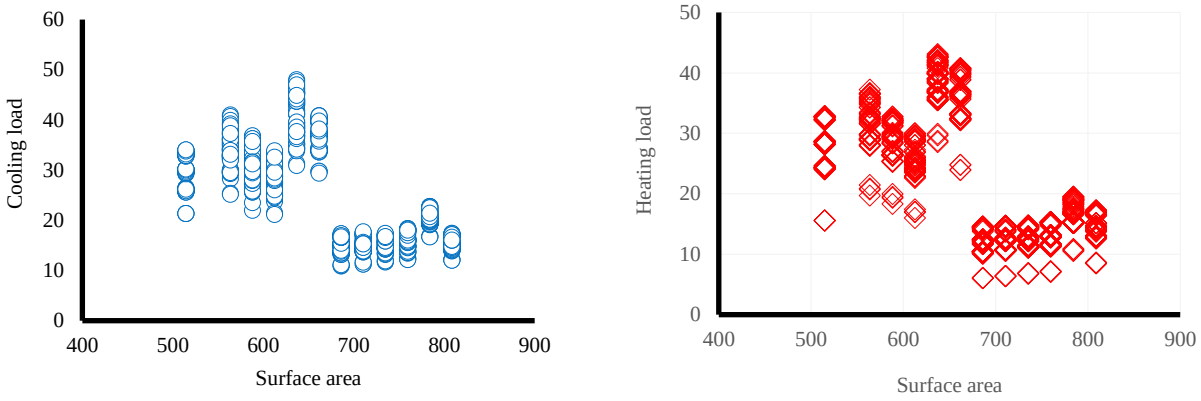

(b) Surface Area

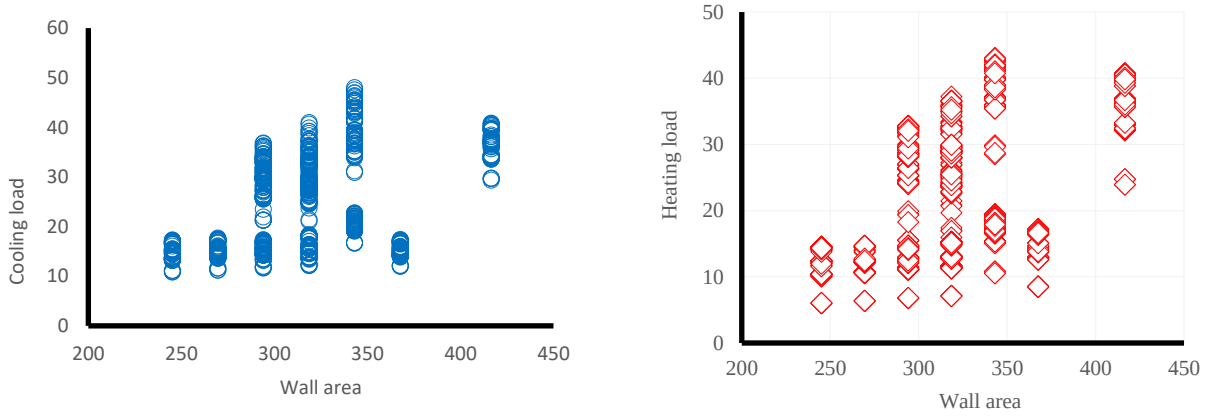

Wall Area

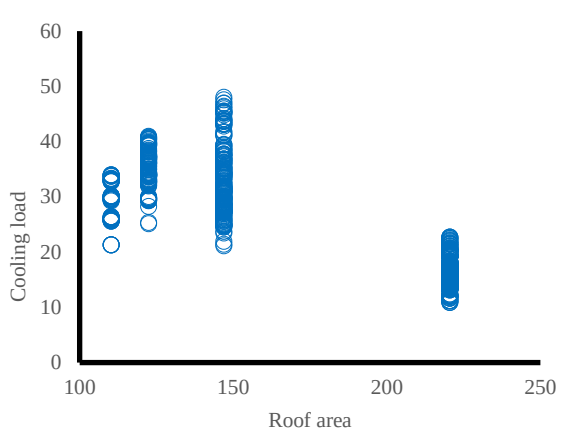

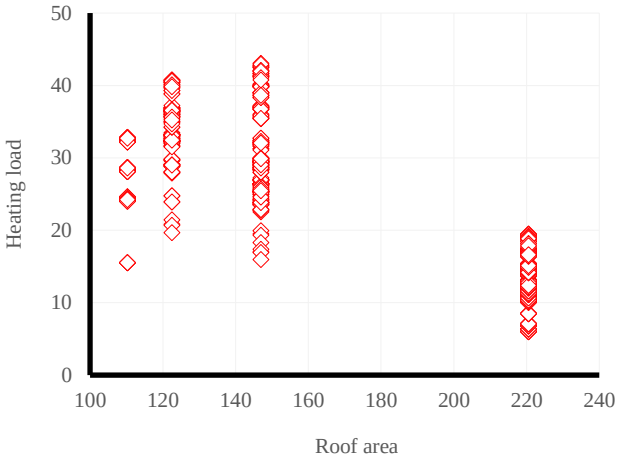

Roof Area

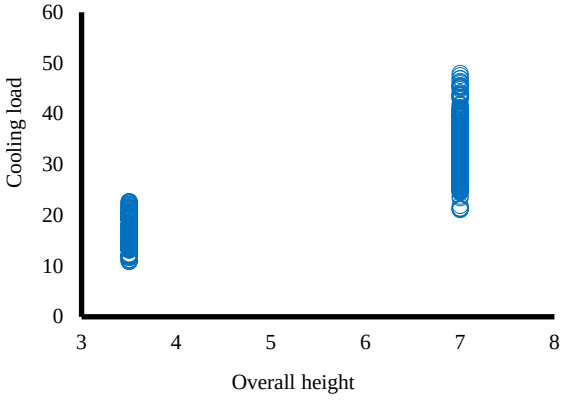

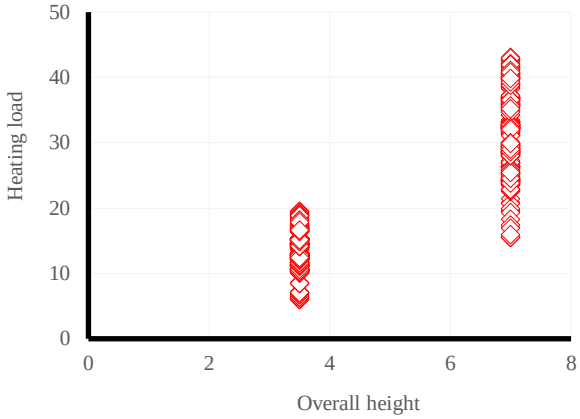

Overall Height

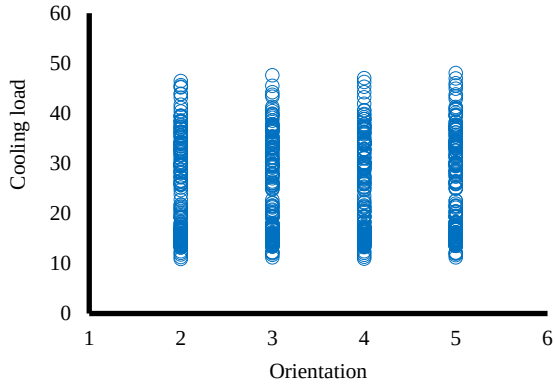

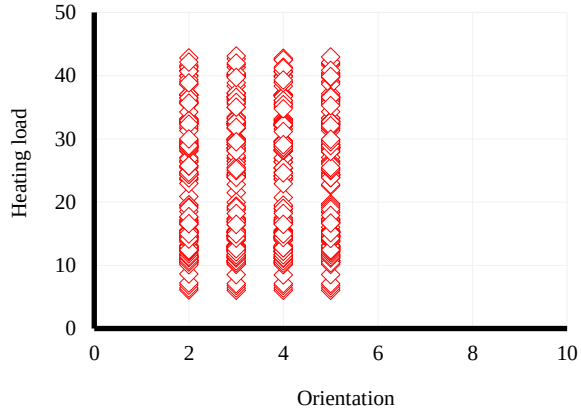

Orientation

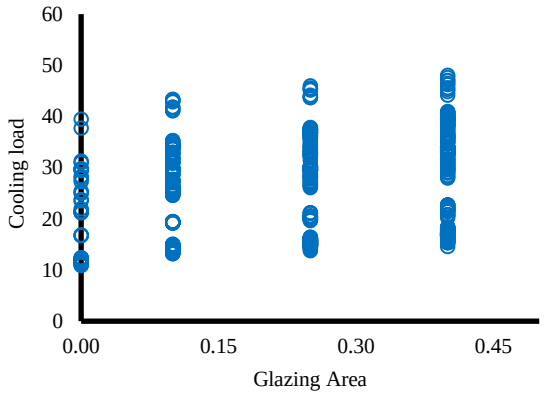

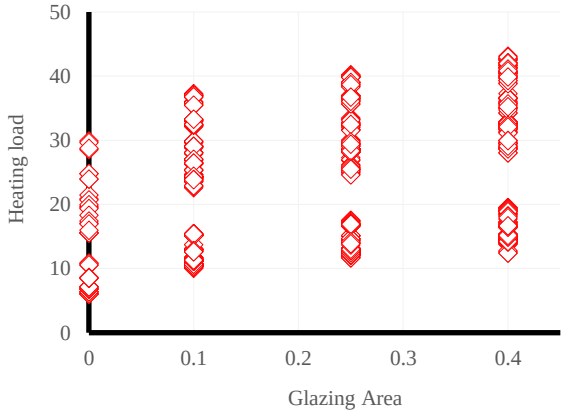

Glazing Area

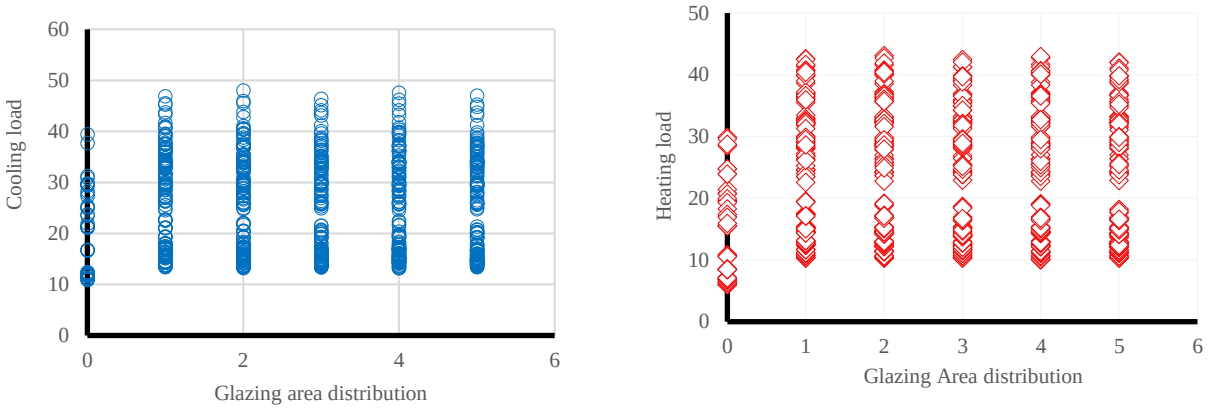

Glazing Area distribution

Figure 5: The graphical description between CL and main influential factors.

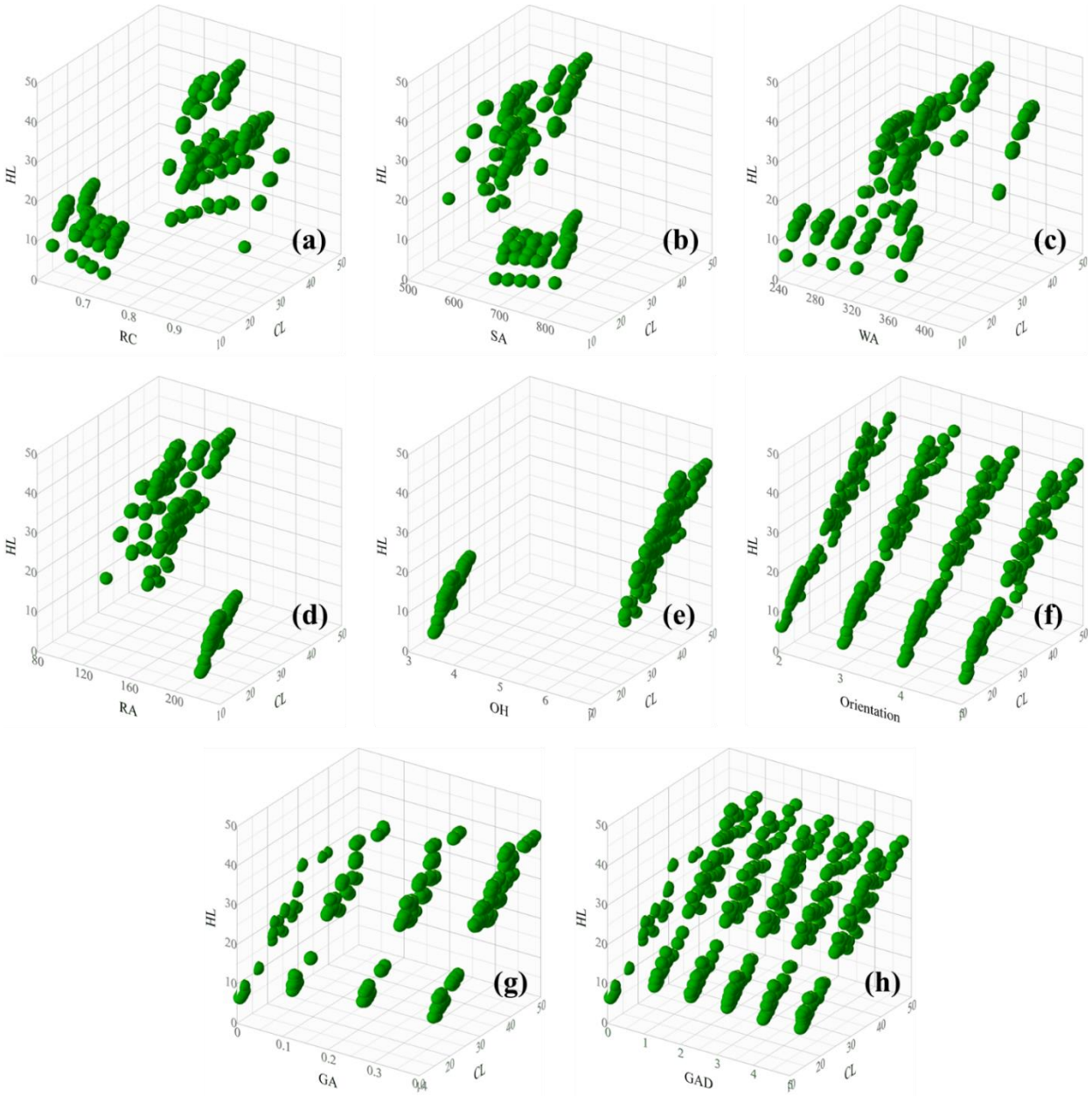

Figure 6: Spatial distribution of inputs variables versus both HL and CL outputs.

Table 1. Descriptive statistical indexes versus the used features

Features	Descriptive index								
	Mean	Standard Error	Median	Mode	Standard Deviation	Sample Variance	Skewness	Minimum	Maximum
Relative Compactness	0.76	0.00	0.75	0.98	0.11	0.01	0.50	0.62	0.98
Roof Area	176.60	1.63	183.75	220.50	45.17	2039.96	-0.16	110.25	220.50
Surface Area	671.71	3.18	673.75	514.50	88.09	7759.16	-0.13	514.50	808.50
Wall Area	318.50	1.57	318.50	294.00	43.63	1903.27	0.53	245.00	416.50
Orientation	3.50	0.04	3.50	2.00	1.12	1.25	0.00	2.00	5.00
Glazing Area distribution	2.81	0.06	3.00	1.00	1.55	2.41	-0.09	0.00	5.00
Overall Height	5.25	0.06	5.25	7.00	1.75	3.07	0.00	3.50	7.00
Glazing Area	0.23	0.00	0.25	0.10	0.13	0.02	-0.06	0.00	0.40

5 Results and discussion

This investigation aimed to predict HLs and CLs in buildings utilizing artificial intelligence according to predictive tools. In the case of an ANN multilayer perceptron (MLP) is employed to estimate the HLs and CLs. The prepared datasets are parted within two sections of the training and testing model. The first section that is selected using 70% of the whole database is considered for the training the ANN models (named training dataset) while the 30 % remained items set to be used for evaluation of their network performances (called testing dataset). The new testing dataset (i.e., selected in each stage of the network simulation) is built using data that varies from the training step. Two statistical indices of determination coefficient (R^2) and root mean square error (RMSE) is employed to compute the network error efficiency and the regression among the target values and system outcomes of HLs and CLs. The upper mentioned indices are significantly utilized and also are presented by Equations 14 and 15, respectively.

$$RMSE = \sqrt{\frac{1}{N}\sum_{i=1}^{N}[(Y_{i_{actual}} - Y_{i_{produced}})]^2} \quad (13)$$

$$R^2 = 1 - \frac{\sum_{j=1}^{N}\left[(Y)_{actual,j} - (Y)_{produced,j}\right]^2}{\sum_{j=1}^{N}\left[(Y)_{actual,j} - (Y)_{mean}\right]^2} \quad (14)$$

where, $Y_{i\ actual}$, $Y_{i\ produced}$, and Y_{mean} indicates values considered in each step of the simulation for the exact, predicted, and the mean values of showed P_{ult}, respectively. Besides, the factor N displays the number of datasets.

5.1 Optimization of MLP models

The effectiveness of several multilayer perceptron-based networks was assessed in this section. In a multilayer perceptron-based networks model, the neurons number for the output and also input layers is taken constantly. Such a number is normally considered to

be equal to the number of output and inputs, respectively. It is important to know that the neurons number in the hidden layer is a different factor that changes relying on the amount of user data. So, in this step and to create a strong multilayer perceptron-based networks structure eight different networks were taken into consideration. Also, for more trustworthiness, the calculation of each of the proposed multilayer perceptron-based networks was repeated six times, and totally, forty-eight various structures were built to specify the most proper structure. Figure 7 shows the results of considered analysis (i.e., respectively, for the R^2 and RMSE, respectively). This trial and error procedure can help to determine the most structure of the optimized network. As seen, to predict the P_{ult} of the considered footing, the best structure of the MLP model with having the minimum error may be achieved while the neurons number in each hidden layer is identical to 5. Accordingly, to have a simplified solution and as shown in Figure 7, the number of nodes equal to five was selected as the best possible neuron number that requires to be chosen in the hidden layers. This will help to find a strong multilayer perceptron-based network structure, which in this section obtained to be 4×5×1 (i.e., four input layers, five neurons in a single hidden layer, and one output layer which is P_{ult}). It should be noted that in the last part of the present work, various reduced formulas are specified according to changes done on the nodes number in a single hidden layer.

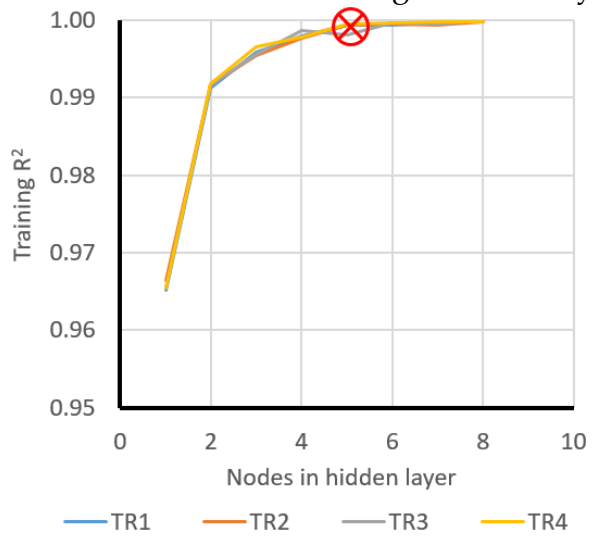

(a)

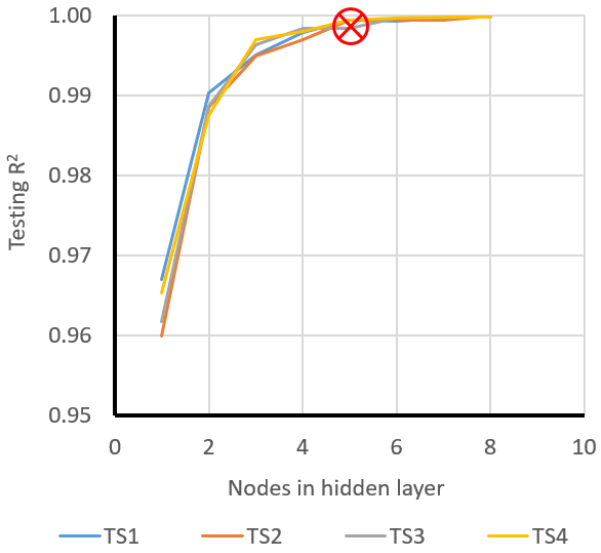

(b)

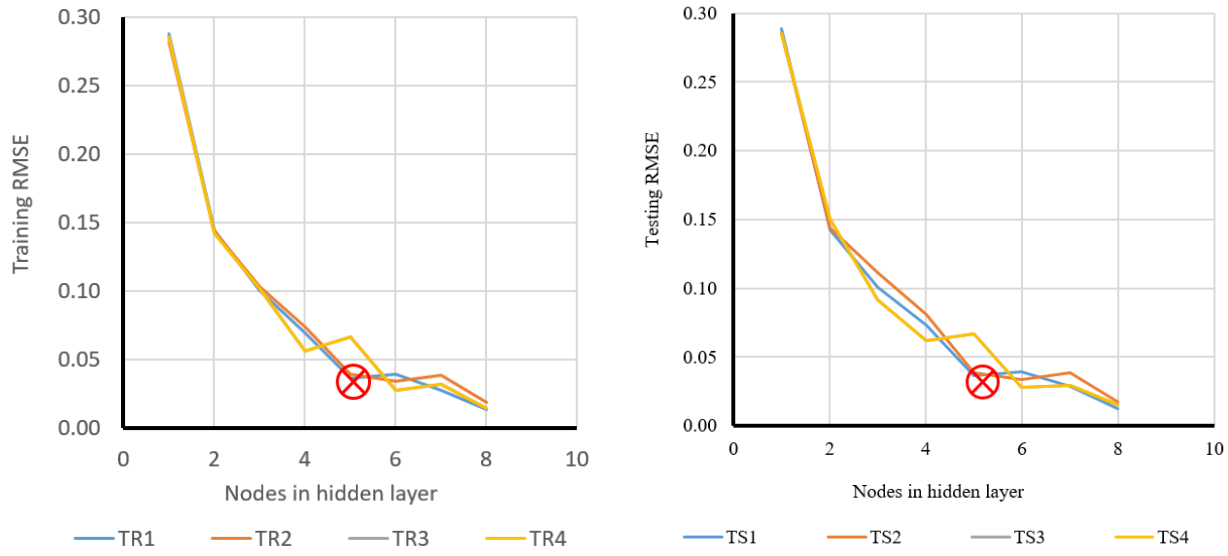

(c) (d)

Figure 7. sensitivity analysis of the R^2 and RMSE of various suggested MLP predict P_{ult}.

The mathematical-based equation of the best-fit MLP structure was considered to the GOA, WDO, and BBO optimization algorithms. Next step consists of selecting the proper cost function, object function, and assessment techniques (e.g., R^2 and RMSE). In this step we try to provide the best-fit relationships between the actual and predicted. In current study a simultaneously two target simulation based were provided for both HLs and CLs. As described, at the end of each iteration the value of cost function is taken to assess the accuracy of the proposed model. In this sense, a sensitivity analysis was then performed for all proposed models of GOA-MLP and WDO-MLP based on the number of population size (also known as swarm size). It is one of the most critical terms through the hybrid intelligent algorithms. Therefore, the hybrid predictive networks are assessed according to various swarm sizes (e.g., in this study, nine sets of swarm sizes were used), leading to 11000 iterations for every one of the proposed hybrid solutions. The swarm size varied between 25 to 500 as shown in Figure 8. All the algorithms conducted 1000 iterations to find enough chances to decrease the rate of errors shown here as mean square error. The convergence curves that are shown in Figure 8 are the first result of the fitness function after the swarm size sensitivity analysis. This part is also called the convergence analysis. As depicted in Figure 8, a-c, respectively, for the GOA-MLP, WDO-MLP and BBO-MLP ensembles, the higher iterations normally caused to decrease in the rate of MSE errors. Besides, nonlinear swarm-based analysis for the estimation of the GOA-MLP, WDO-MLP and BBO-MLP of heating load in energy-efficient buildings are tabulated in Tables 2-4, respectively.

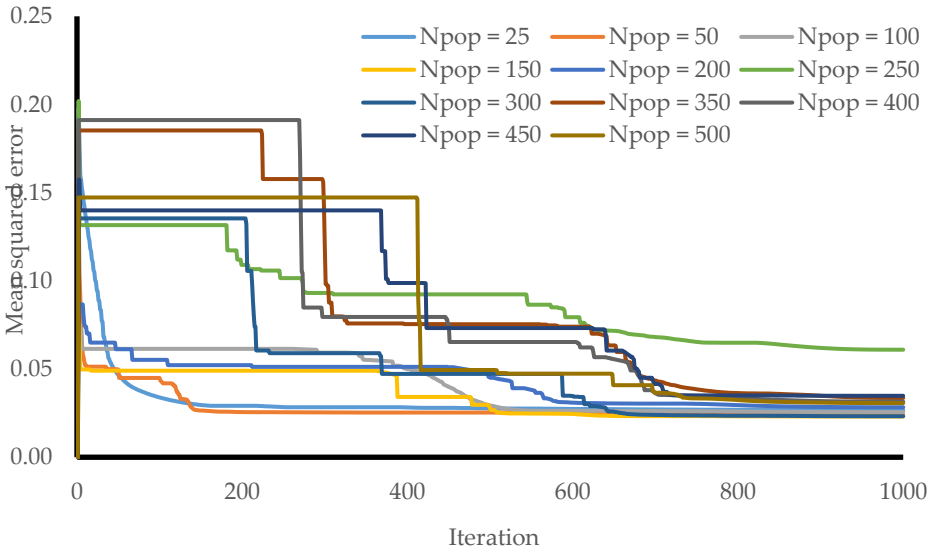

(a)

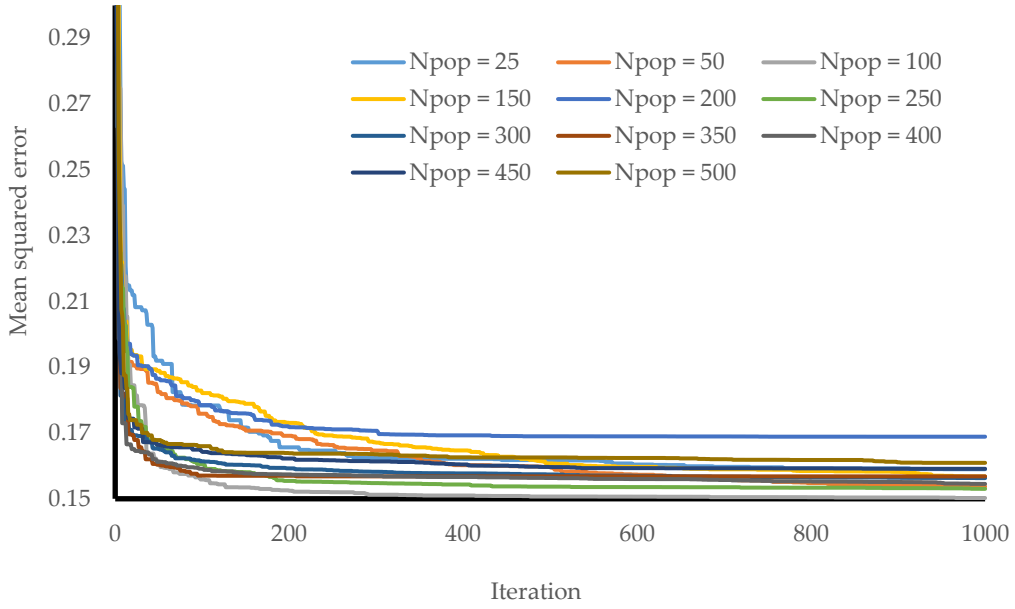

(b)

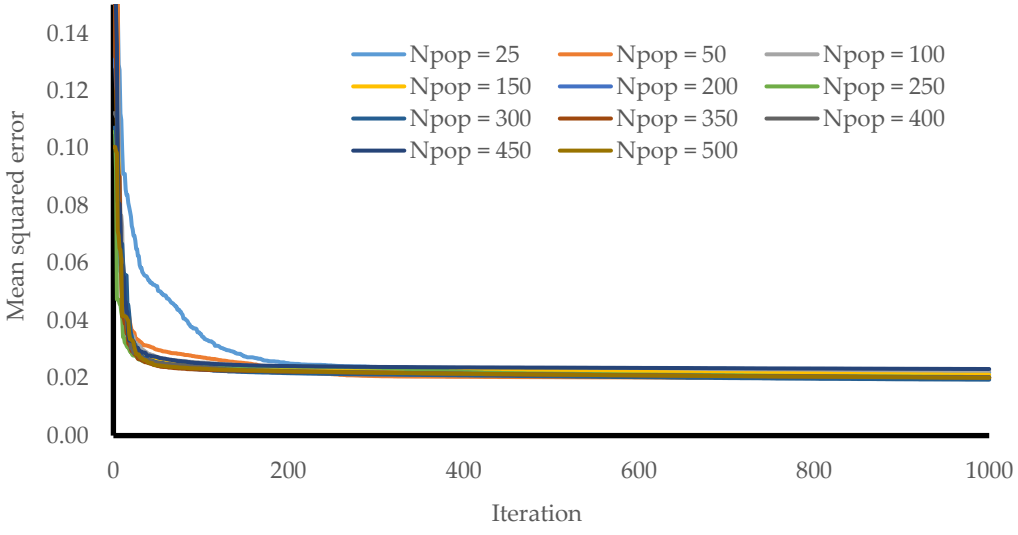

(c)

Figure 8: Executed population-based sensitivity analysis for the (a) GOA-MLP, and (b) WDO-MLP, (c) BBO-MLP

Table 2: Nonlinear GOA-MLP swarm-based analysis for the estimation of the heating load

Population size	Network result				Ranking				Total rank	RANK
	Train		Test		Train		Test			
	R^2	RMSE	R^2	RMSE	R^2	RMSE	R^2	RMSE		
25	0.999	0.152	0.999	0.151	6	4	6	3	**19**	7
50	0.997	0.147	0.998	0.148	3	6	3	4	**16**	9
100	0.999	0.146	0.999	0.154	7	8	7	2	**24**	5
150	1.000	0.153	1.000	0.147	9	2	9	6	**26**	4
200	1.000	0.144	1.000	0.139	10	9	10	9	**38**	2
250	0.997	0.146	0.996	0.147	1	7	1	7	**16**	9
300	0.998	0.156	0.998	0.158	4	1	5	1	**11**	11
350	0.999	0.149	0.999	0.144	8	5	8	8	**29**	3
400	0.998	0.153	0.998	0.148	5	3	4	5	**17**	8
450	0.997	0.142	0.997	0.135	2	10	2	10	**24**	5
500	1.000	0.044	1.000	0.043	11	11	11	11	**44**	1

Table 3: Nonlinear WDO-MLP swarm-based analysis for the estimation of the heating load

Population size	Network result				Ranking				Total rank	RANK
	Train 2		Test 2		Train 2		Test 2			
	R^2	RMSE	R^2	RMSE	R^2	RMSE	R^2	RMSE		
25	0.999	0.154	0.999	0.152	6	3	5	4	**18**	8
50	1.000	0.154	0.999	0.156	10	4	8	3	**25**	6
100	0.996	0.150	0.997	0.160	1	7	1	1	**10**	10
150	1.000	0.138	1.000	0.140	11	11	11	11	**44**	1
200	0.999	0.151	0.999	0.146	8	5	10	7	**30**	3
250	0.998	0.154	0.998	0.160	2	2	2	2	**8**	11
300	0.999	0.158	0.999	0.150	9	1	9	5	**24**	7
350	0.999	0.151	0.998	0.149	3	6	3	6	**18**	8
400	0.999	0.146	0.999	0.141	7	10	6	9	**32**	2
450	0.999	0.148	0.999	0.144	4	8	7	8	**27**	5
500	0.999	0.147	0.999	0.140	5	9	4	10	**28**	4

Table 4: Nonlinear BBO-MLP swarm-based analysis for the estimation of the heating load

Population size	Network result				Ranking				Total rank	RANK
	Train		Test		Train		Test			
	R^2	RMSE	R^2	RMSE	R^2	RMSE	R^2	RMSE		
25	0.999	0.151	0.998	0.147	4	4	2	8	**18**	9
50	0.998	0.152	0.999	0.157	2	1	3	1	**7**	11
100	0.999	0.145	0.999	0.146	7	11	7	10	**35**	1
150	0.997	0.147	0.997	0.154	1	10	1	2	**14**	10
200	1.000	0.150	1.000	0.151	9	5	9	4	**27**	4
250	1.000	0.148	1.000	0.149	10	9	10	6	**35**	1
300	0.999	0.152	0.999	0.153	8	2	8	3	**21**	8
350	0.999	0.151	0.999	0.141	6	3	6	11	**26**	5
400	0.999	0.150	0.999	0.147	3	6	5	9	**23**	6
450	1.000	0.149	1.000	0.149	11	8	11	5	**35**	1
500	0.999	0.149	0.999	0.148	5	7	4	7	**23**	6

5.2 Assessment of the proposed models

The reliability of the proposed models is assessed by evaluating the measured and predicted values of HLs and CLs. Two different sets of error criteria of MSE and RMSE is used to have an estimation of the error as well as checking the performance of samples obtained from both training and testing datasets. It is worth to note that the output fitness from both of the training and testing phases defines the generalization power and training capability, respectively. The computed training and testing values in the simultaneous HL&CL prediction for GOA-MLP, WOA-MLP, and BBO-MLP techniques are presented in Figures 9 and 10, respectively. The computed error values in the simultaneous HL&CL prediction for GOA-MLP, WOA-MLP, and BBO-MLP techniques are also shown in Figure 11. Figures 12 (which is referred to GOA-MLP) and 13 (that is referred to WDO-MLP) displays a graphical evaluation between the original predicted and measured patterns of the heating and cooling loads (for both of the training and testing datasets). Similarly, the accuracy of the proposed multitarget prediction BBO-MLP techniques is shown in Figure 14. As is seen, all proposed models result in a valid estimate of the HLs and CLs patterns. The calculated R^2 (training =0.9529, testing = 0.9512) for the GOA-MLP-HLs and R^2 of (training = 0.9998, testing = 0.9998) for the CLs estimation. In the case of WDO-MLP-HLs, the R^2 (training =0.9551 and testing = 0.9464) while for the WDO-MLP-CLs, the R^2 (training = 0.9995 and testing = 0.9994) were found. Lastly, for the case of BBO-MLP-HLs, the R^2 (training = 0.9563 and testing = 0.943) and BBO-MLP-CLs, the R^2 (training = 0.9981 and testing = 0.9975) were calculated. Considering the three proposed techniques and after performing a nonlinear swarm optimization process, it can be seen that the best-fit model is obtained from the proposed structure of WDO-MLP. The result from the accuracy also shows excellent accuracy, and this proved the WDO-MLP is the most effectual hybrid techniques in training the MLP.

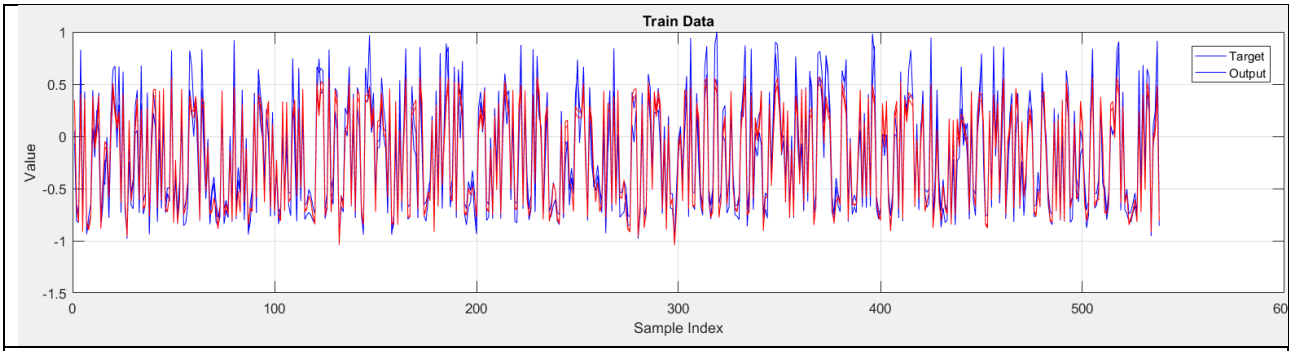

(a) GOA-MLP-Training

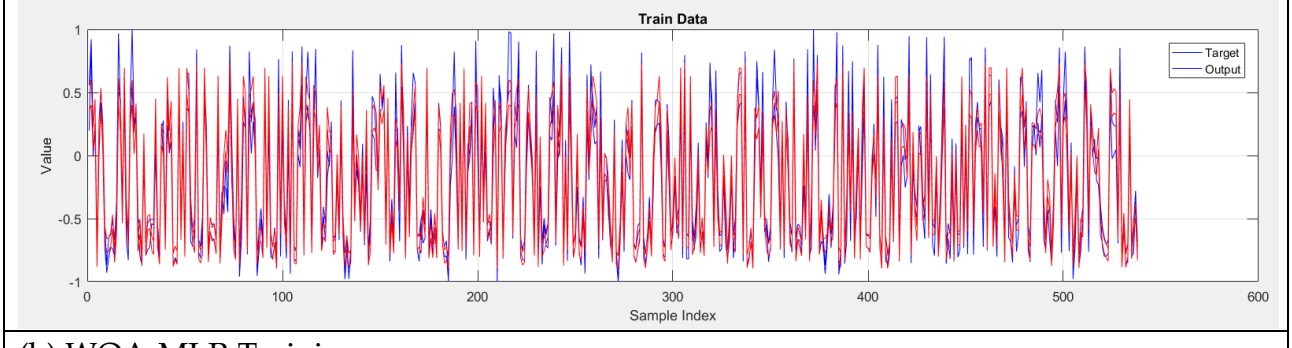

(b) WOA-MLP-Training

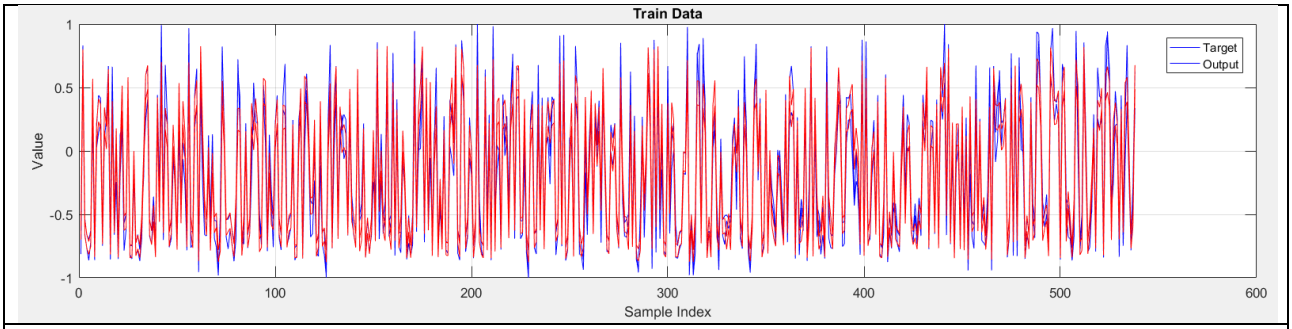

(c) BBO-MLP-Training

Figure 9: The computed training values in the simultaneous HL&CL prediction for (a) GOA-MLP, (b) WOA-MLP, (c) BBO-MLP.

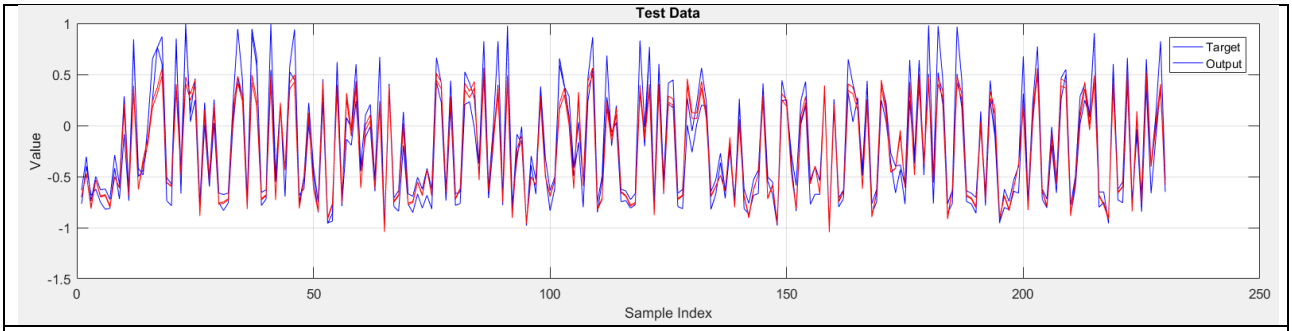

(a) GOA-MLP-Testing

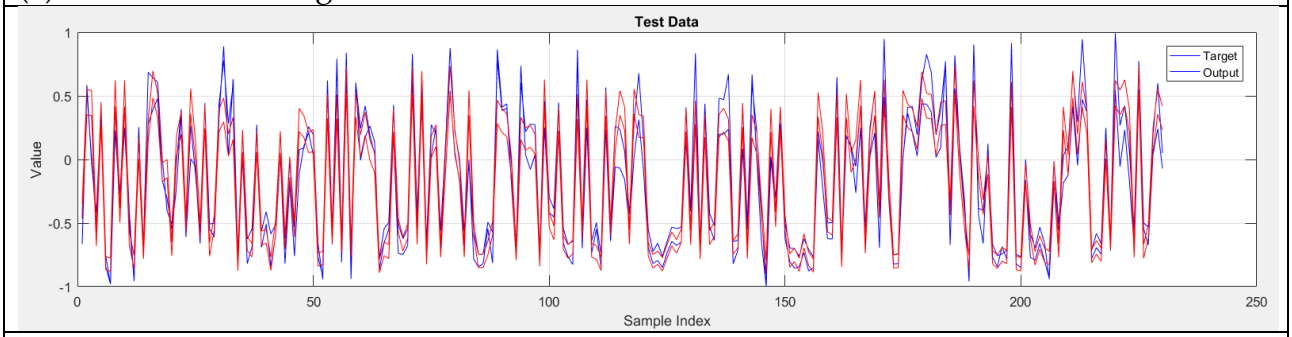

(b) WOA-MLP- Testing

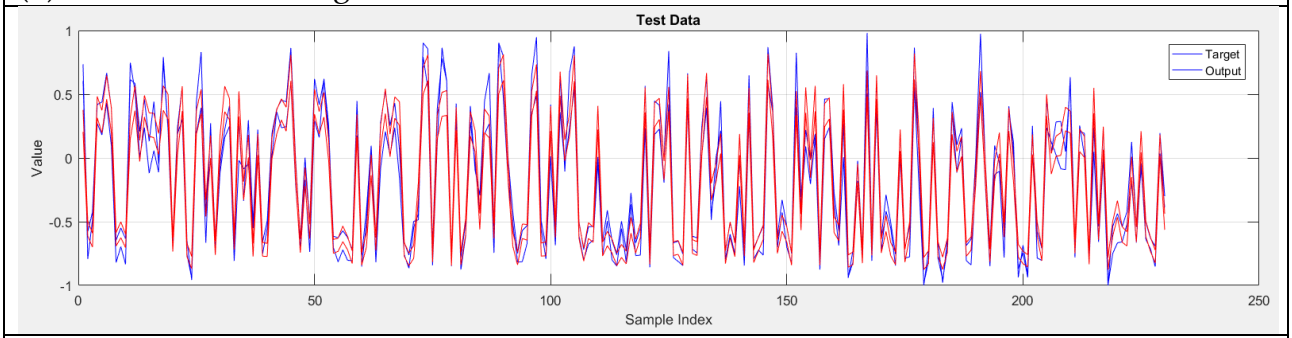

(c) BBO-MLP- Testing

Figure 10: The computed Testing values in the simultaneous HL&CL prediction for (a) GOA-MLP, (b) WOA-MLP, (c) BBO-MLP.

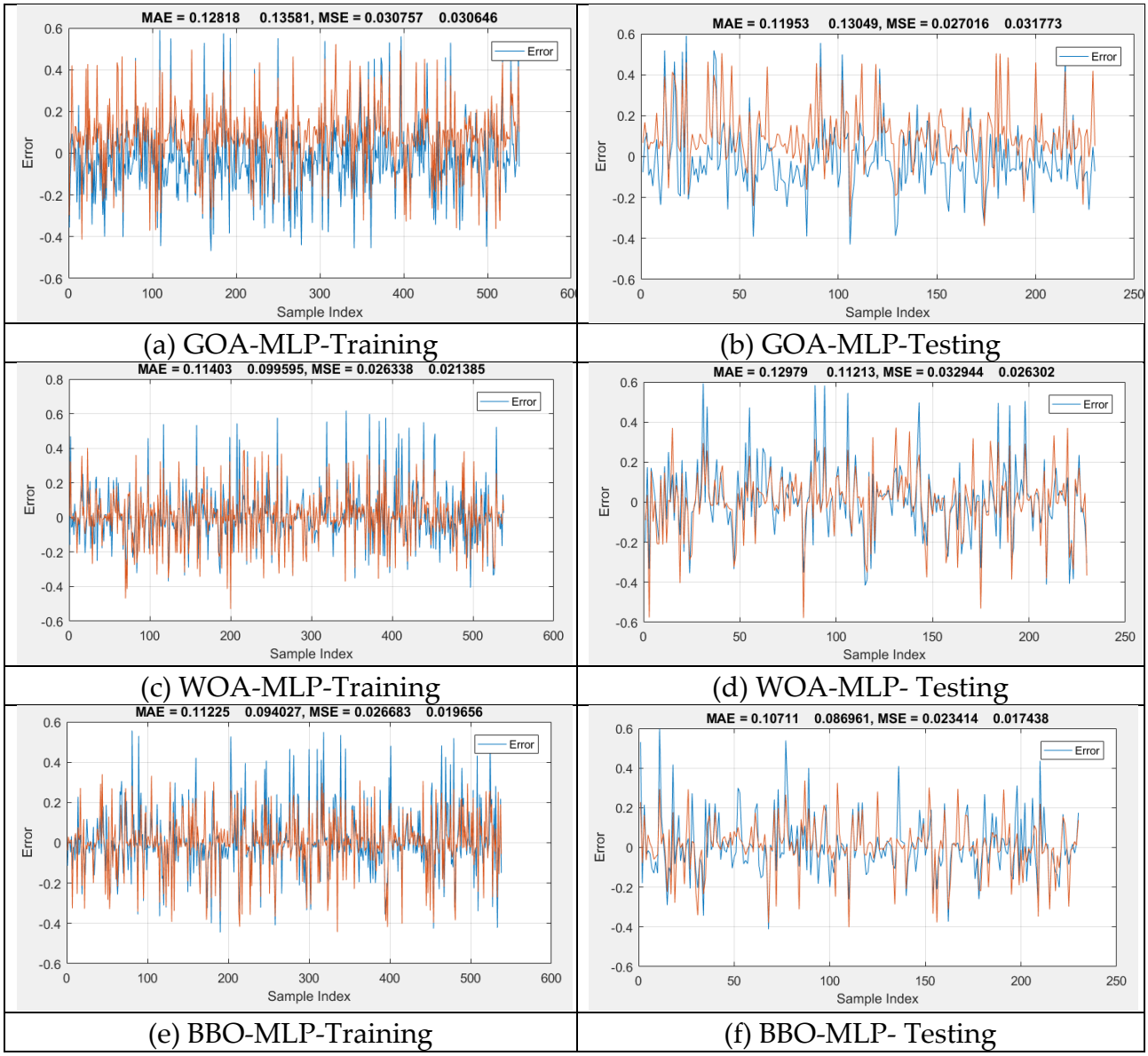

Figure 11: The computed error values in the simultaneous HL&CL prediction for (a) GOA-MLP, (b) WOA-MLP, (c) BBO-MLP.

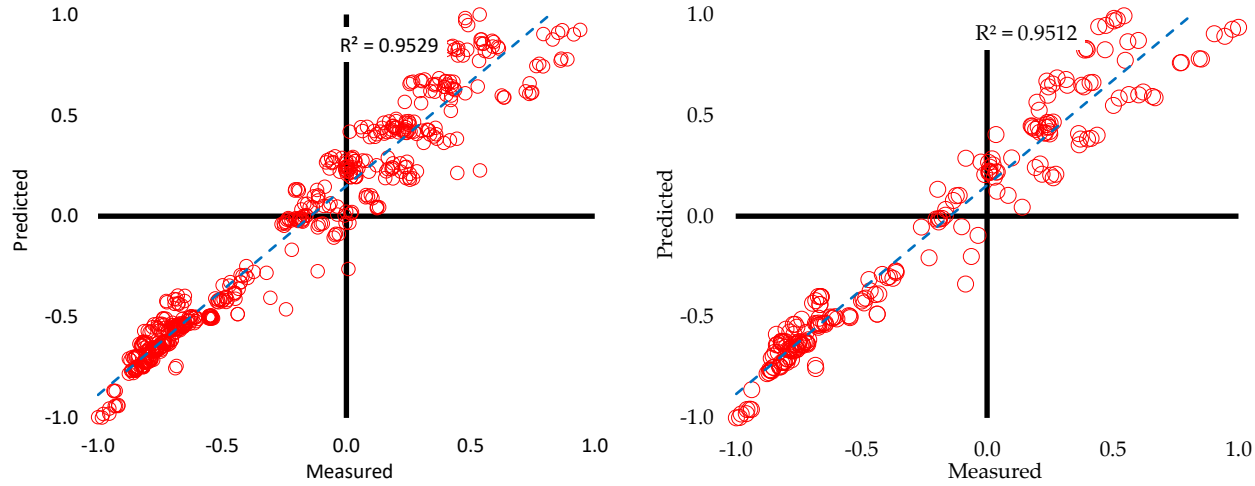

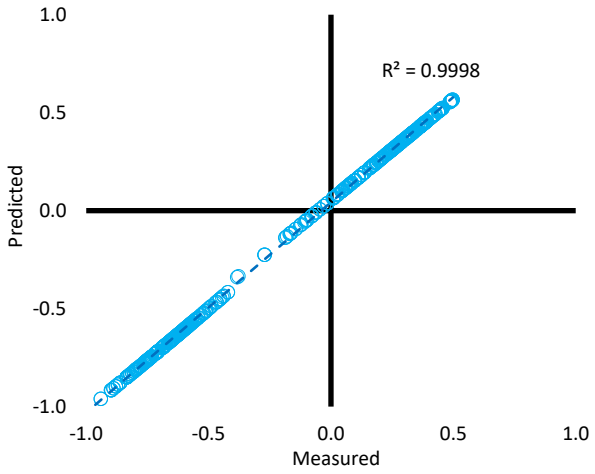

(c) GOA-MLP training for cooling load estimation

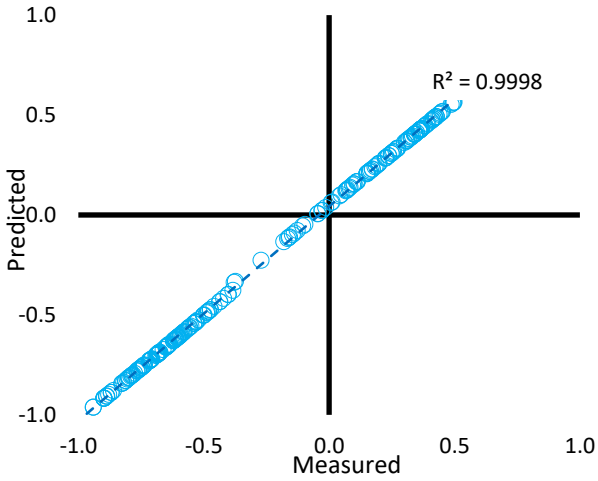

(d) GOA-MLP testing for cooling load estimation

Figure 12: The graphical results of GOA-MLP technique between the actual heating and cooling loads

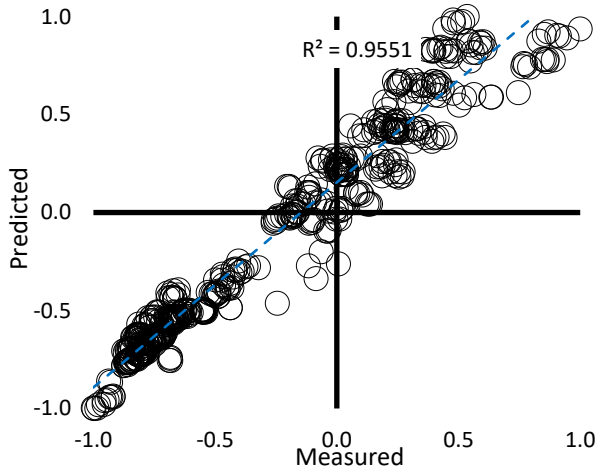

(a) WDO -MLP training for heating load estimation

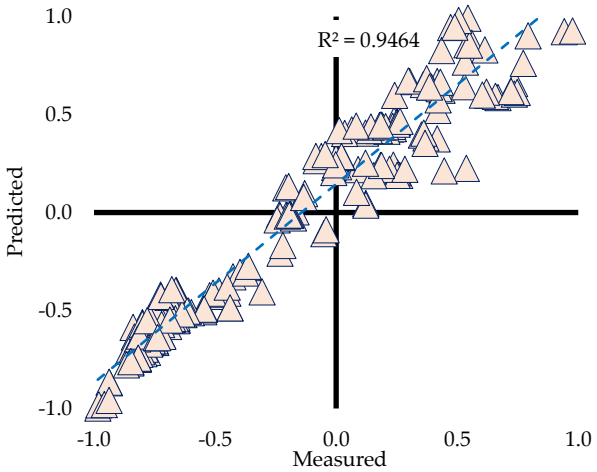

(b) WDO -MLP testing for heating load estimation

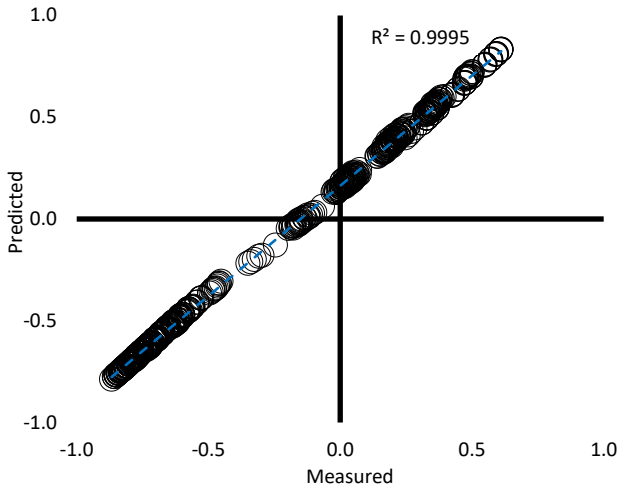

(c) WDO -MLP training for cooling load estimation

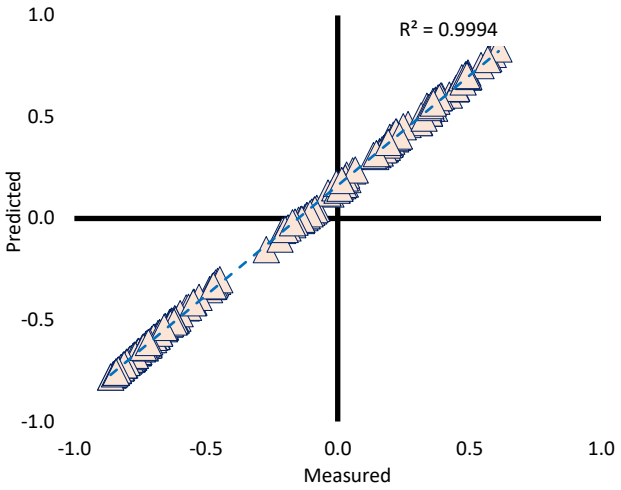

(d) WDO -MLP testing for cooling load estimation

Figure 13: The graphical results of WDO-MLP technique between the actual heating and cooling loads

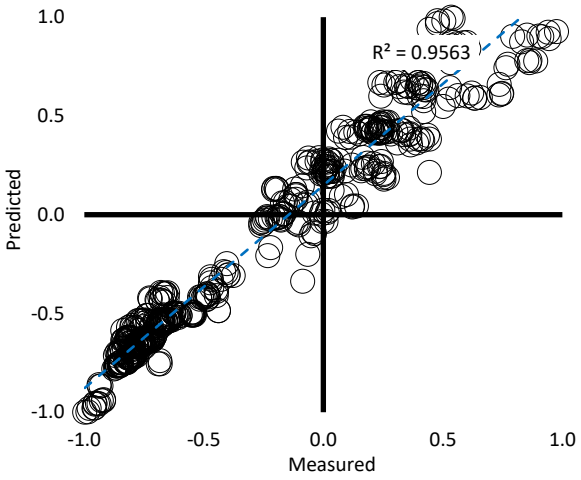

(a) BBO -MLP training for heating load estimation

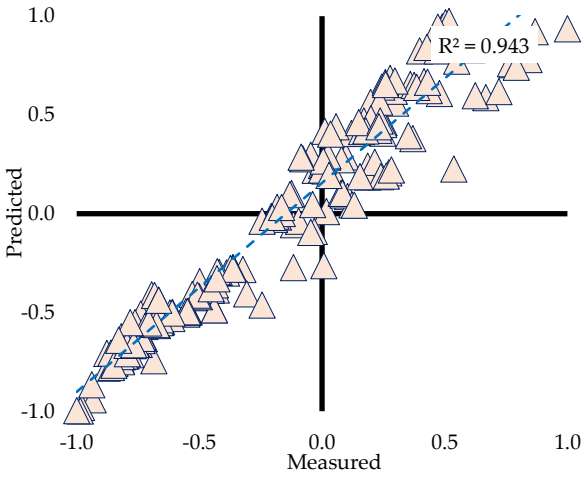

(b) BBO -MLP testing for heating load estimation

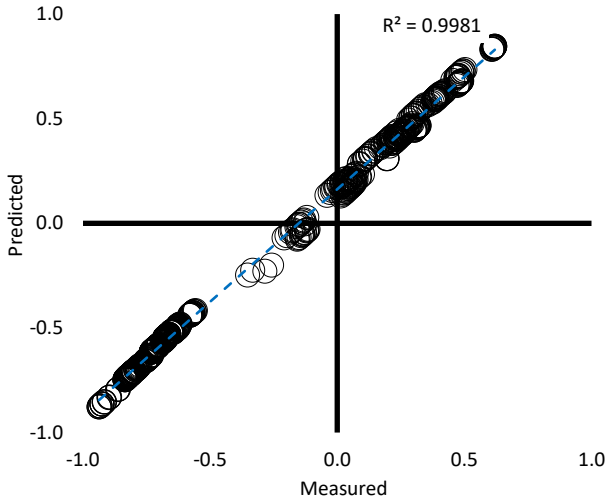

(c) BBO -MLP training for cooling load estimation

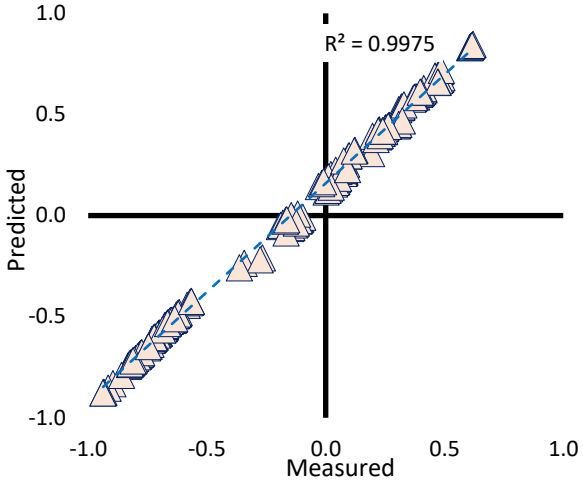

(d) BBO -MLP testing for cooling load estimation

Figure 14: The graphical results of BBO-MLP technique between the actual heating and cooling loads

5.3 Simplified multitarget equation

To have a more practical formula that can be used to predict both HLs and CLs and considering the minimum required error, in this section, the two node-based (having one single hidden layer) is provided. Also, to have a better understanding, the MLP-best-fit equation is prepared according to the optimized weights and biases. These terms are unique for any particular database. Noting that to have practical use of this formula, the well-known mathematical function of Tangent-Sigmoid (*Tansig*) is also provided. *Tansig* is also called the MLP activation function. The *Tansig* equation expressed by Equation 16. The R^2 accuracy of the proposed formula for prediction of multi targets of HLs and CLs simultaneously were 0.98547, 0.9866, 0.98374 for the training, testing and validation datasets, respectively.

$$\begin{aligned} HL &= -0.2809 \times Y1 \quad 0.0008 \times Y2 \quad -0.4820 \\ CL &= -0.9463 \times Y2 \quad 0.6540 \times Y3 \quad -0.9082 \end{aligned} \tag{15}$$

HL-Y1 = Tansig(0.6288 ×A+0.1026 × B+0.8159×C+0.6752×D-0.4539×E-0.5838× F-0.130458198 × G-0.2809
HL-Y2 = Tansig(-0.3145 × A-0.2015 × B+0.3191 × C-0.7065 × D+0.4849 × E-0.8442 × F+0.79155 × G-0.9463
CL-Y1 = Tansig(0.6288 × A+0.1026 × B+0.8159 × C+0.6752 × D-0.4539 × E-0.5838 × F-0.1305 × G+0.0008
CL-Y2 = Tansig(-0.3145 × A-0.2015 × B+0.3191 × C-0.7065 × D+0.4849 × E-0.8442 × F+0.7916 × G+0.6540

6 Conclusions

This article concerned with the multitarget calculation of HLs and Cls of residential buildings through the HVAC system design simultaneously. To limit the drawbacks of MLP technique, the hybrid intelligent techniques are implemented. The focus of the three proposed models abbreviated as GOA-MLP, WDO-MLP, and BBO-MLP was to introduce several reliable novel hybrid models to simulate both HLs and CLs. Overall, and after 33000

iterations of the three proposed algorithms, the behavior of each method (e.g., to optimize the performance of the selected MLP structure) are evaluated. To this end, the GOA, WDO, and BBO were combined with a conventional MLP to develope the GOA-MLP, WDO-MLP, and BBO-MLP ensemble. Both of the chosen targets linked to their influential input parameters; however, the obtained accuracy results for the CLs are calculated with higher accuracy. Since the CLs prediction was almost equal to the real values, the main comparison was made based on the values of predicted HLs. As a result, the WDO-MLP found to be the most efficient hybrid algorithm in optimizing the MLP. The WDO-MLP followed by GOA-MLP and BBO-MLP.

7 References

1. US EIA *Total energy. Annual Energy Review. U.S. Department of Energy (DOE). https://www.eia.gov/totalenergy/data/annual/index.php.*; United States Energy Information Administration (US EIA), Accessed 10 Nov 2017., 2017.
2. IEA, International Energy Agency. Key World Energy Statistics. 2015.
3. Zhou, Y. K.; Zheng, S. Q.; Zhang, G. Q., Artificial neural network based multivariable optimization of a hybrid system integrated with phase change materials, active cooling and hybrid ventilations. *Energy Conv. Manag.* **2019,** 197, 19.
4. Ahmad, A. S.; Hassan, M. Y.; Abdullah, M. P.; Rahman, H. A.; Hussin, F.; Abdullah, H.; Saidur, R., A review on applications of ANN and SVM for building electrical energy consumption forecasting. *Renew. Sust. Energ. Rev.* **2014,** 33, 102-109.
5. Mocanu, E.; Nguyen, P. H.; Gibescu, M.; Kling, W. L., Deep learning for estimating building energy consumption. *Sustain. Energy Grids Netw.* **2016,** 6, 91-99.
6. Xu, M.; Li, T.; Wang, Z.; Deng, X.; Yang, R.; Guan, Z., Reducing Complexity of HEVC: A Deep Learning Approach. *IEEE Transactions on Image Processing* **2018,** 27, (10), 5044-5059.
7. Li, T.; Xu, M.; Zhu, C.; Yang, R.; Wang, Z.; Guan, Z., A Deep Learning Approach for Multi-Frame In-Loop Filter of HEVC. *IEEE Transactions on Image Processing* **2019,** 28, (11), 5663-5678.
8. Qiu, T.; Shi, X.; Wang, J.; Li, Y.; Qu, S.; Cheng, Q.; Cui, T.; Sui, S., Deep Learning: A Rapid and Efficient Route to Automatic Metasurface Design. *Advanced Science* **2019,** 6, (12), 1900128.
9. Chen, H.; Chen, A.; Xu, L.; Xie, H.; Qiao, H.; Lin, Q.; Cai, K., A deep learning CNN architecture applied in smart near-infrared analysis of water pollution for agricultural irrigation resources. *Agricultural Water Management* **2020,** 240, 106303.
10. Lv, Z.; Qiao, L., Deep belief network and linear perceptron based cognitive computing for collaborative robots. *Applied Soft Computing* **2020,** 92, 106300.
11. Qian, J.; Feng, S.; Li, Y.; Tao, T.; Han, J.; Chen, Q.; Zuo, C., Single-shot absolute 3D shape measurement with deep-learning-based color fringe projection profilometry. *Optics Letters* **2020,** 45, (7), 1842-1845.
12. Qian, J.; Feng, S.; Tao, T.; Hu, Y.; Li, Y.; Chen, Q.; Zuo, C., Deep-learning-enabled geometric constraints and phase unwrapping for single-shot absolute 3D shape measurement. *APL Photonics* **2020,** 5, (4), 046105.
13. Liu, S.; Chan, F. T. S.; Ran, W., Decision making for the selection of cloud vendor: An improved approach under group decision-making with integrated weights and objective/subjective attributes. *Expert Systems with Applications* **2016,** 55, 37-47.
14. Wu, C.; Wu, P.; Wang, J.; Jiang, R.; Chen, M.; Wang, X., Critical review of data-driven decision-making in bridge operation and maintenance. *Structure and Infrastructure Engineering* **2020**, 1-24.

15. Cao, B.; Zhao, J.; Lv, Z.; Gu, Y.; Yang, P.; Halgamuge, S. K., Multiobjective Evolution of Fuzzy Rough Neural Network via Distributed Parallelism for Stock Prediction. *IEEE Transactions on Fuzzy Systems* **2020,** 28, (5), 939-952.
16. Quan, Q.; Hao, Z.; Xifeng, H.; Jingchun, L., Research on water temperature prediction based on improved support vector regression. *Neural Computing and Applications* **2020**, 1-10.
17. Shi, K.; Wang, J.; Tang, Y.; Zhong, S., Reliable asynchronous sampled-data filtering of T–S fuzzy uncertain delayed neural networks with stochastic switched topologies. *Fuzzy Sets and Systems* **2020,** 381, 1-25.
18. Shi, K.; Wang, J.; Zhong, S.; Tang, Y.; Cheng, J., Non-fragile memory filtering of T-S fuzzy delayed neural networks based on switched fuzzy sampled-data control. *Fuzzy Sets and Systems* **2020,** 394, 40-64.
19. Zhu, Q., Research on Road Traffic Situation Awareness System Based on Image Big Data. *IEEE Intelligent Systems* **2020,** 35, (1), 18-26.
20. Zhao, X.; Ye, Y.; Ma, J.; Shi, P.; Chen, H., Construction of electric vehicle driving cycle for studying electric vehicle energy consumption and equivalent emissions. *Environmental Science and Pollution Research* **2020**, 1-15.
21. Zhang, T.; Wu, X.; Li, H.; Tsang, D. C. W.; Li, G.; Ren, H., Struvite pyrolysate cycling technology assisted by thermal hydrolysis pretreatment to recover ammonium nitrogen from composting leachate. *Journal of Cleaner Production* **2020,** 242, 118442.
22. Zhang, K.; Ruben, G. B.; Li, X.; Li, Z.; Yu, Z.; Xia, J.; Dong, Z., A comprehensive assessment framework for quantifying climatic and anthropogenic contributions to streamflow changes: A case study in a typical semi-arid North China basin. *Environmental Modelling & Software* **2020,** 128, 104704.
23. Yang, W.; Zhao, Y.; Wang, D.; Wu, H.; Lin, A.; He, L., Using Principal Components Analysis and IDW Interpolation to Determine Spatial and Temporal Changes of Surface Water Quality of Xin'anjiang River in Huangshan, China. *International Journal of Environmental Research and Public Health* **2020,** 17, (8), 2942.
24. Wang, Y.; Yuan, Y.; Wang, Q.; Liu, C.; Zhi, Q.; Cao, J., Changes in air quality related to the control of coronavirus in China: Implications for traffic and industrial emissions. *Science of The Total Environment* **2020,** 731, 139133.
25. Wang, S.; Zhang, K.; van Beek, L. P. H.; Tian, X.; Bogaard, T. A., Physically-based landslide prediction over a large region: Scaling low-resolution hydrological model results for high-resolution slope stability assessment. *Environmental Modelling & Software* **2020,** 124, 104607.
26. Liu, J.; Liu, Y.; Wang, X., An environmental assessment model of construction and demolition waste based on system dynamics: a case study in Guangzhou. *Environmental Science and Pollution Research* **2020,** 27, (30), 37237-37259.
27. Jia, L.; Liu, B.; Zhao, Y.; Chen, W.; Mou, D.; Fu, J.; Wang, Y.; Xin, W.; Zhao, L., Structure design of MoS2@Mo2C on nitrogen-doped carbon for enhanced alkaline hydrogen evolution reaction. *Journal of Materials Science* **2020,** 55, (34), 16197-16210.
28. He, L.; Shao, F.; Ren, L., Sustainability appraisal of desired contaminated groundwater remediation strategies: an information-entropy-based stochastic multi-criteria preference model. *Environment, Development and Sustainability* **2020**, 1-21.
29. Chao, L.; Zhang, K.; Li, Z.; Zhu, Y.; Wang, J.; Yu, Z., Geographically weighted regression based methods for merging satellite and gauge precipitation. *Journal of Hydrology* **2018,** 558, 275-289.
30. He, L.; Shao, F.; Ren, L., Sustainability appraisal of desired contaminated groundwater remediation strategies: an information-entropy-based stochastic multi-criteria preference model. *Environment, Development and Sustainability* **2020**.
31. Zhang, T.; He, X.; Deng, Y.; Tsang, D. C. W.; Yuan, H.; Shen, J.; Zhang, S., Swine manure valorization for phosphorus and nitrogen recovery by catalytic–thermal hydrolysis and struvite crystallization. *Science of The Total Environment* **2020,** 729, 138999.

32. Han, X.; Zhang, D.; Yan, J.; Zhao, S.; Liu, J., Process development of flue gas desulphurization wastewater treatment in coal-fired power plants towards zero liquid discharge: Energetic, economic and environmental analyses. *Journal of Cleaner Production* **2020,** 261, 121144.
33. Feng, S.; Lu, H.; Tian, P.; Xue, Y.; Lu, J.; Tang, M.; Feng, W., Analysis of microplastics in a remote region of the Tibetan Plateau: Implications for natural environmental response to human activities. *Science of The Total Environment* **2020,** 739, 140087.
34. Zhang, T.; Wu, X.; Fan, X.; Tsang, D. C. W.; Li, G.; Shen, Y., Corn waste valorization to generate activated hydrochar to recover ammonium nitrogen from compost leachate by hydrothermal assisted pretreatment. *Journal of Environmental Management* **2019,** 236, 108-117.
35. Keshtegar, B.; Heddam, S.; Sebbar, A.; Zhu, S.-P.; Trung, N.-T., SVR-RSM: a hybrid heuristic method for modeling monthly pan evaporation. *Environmental Science and Pollution Research* **2019,** 26, (35), 35807-35826.
36. Hu, X.; Chong, H.-Y.; Wang, X., Sustainability perceptions of off-site manufacturing stakeholders in Australia. *Journal of Cleaner Production* **2019,** 227, 346-354.
37. He, L.; Shen, J.; Zhang, Y., Ecological vulnerability assessment for ecological conservation and environmental management. *Journal of Environmental Management* **2018,** 206, 1115-1125.
38. He, L.; Chen, Y.; Zhao, H.; Tian, P.; Xue, Y.; Chen, L., Game-based analysis of energy-water nexus for identifying environmental impacts during Shale gas operations under stochastic input. *Science of The Total Environment* **2018,** 627, 1585-1601.
39. Zhang, K.; Wang, Q.; Chao, L.; Ye, J.; Li, Z.; Yu, Z.; Yang, T.; Ju, Q., Ground observation-based analysis of soil moisture spatiotemporal variability across a humid to semi-humid transitional zone in China. *Journal of Hydrology* **2019,** 574, 903-914.
40. Chen, Y.; Li, J.; Lu, H.; Yan, P., Coupling system dynamics analysis and risk aversion programming for optimizing the mixed noise-driven shale gas-water supply chains. *Journal of Cleaner Production* **2021,** 278, 123209.
41. Li, X.; Zhang, R.; Zhang, X.; Zhu, P.; Yao, T., Silver-Catalyzed Decarboxylative Allylation of Difluoroarylacetic Acids with Allyl Sulfones in Water. *Chemistry – An Asian Journal* **2020,** 15, (7), 1175-1179.
42. He, L.; Chen, Y.; Li, J., A three-level framework for balancing the tradeoffs among the energy, water, and air-emission implications within the life-cycle shale gas supply chains. *Resources, Conservation and Recycling* **2018,** 133, 206-228.
43. Chen, Y.; He, L.; Li, J.; Zhang, S., Multi-criteria design of shale-gas-water supply chains and production systems towards optimal life cycle economics and greenhouse gas emissions under uncertainty. *Computers & Chemical Engineering* **2018,** 109, 216-235.
44. Cheng, X.; He, L.; Lu, H.; Chen, Y.; Ren, L., Optimal water resources management and system benefit for the Marcellus shale-gas reservoir in Pennsylvania and West Virginia. *Journal of Hydrology* **2016,** 540, 412-422.
45. Yang, M.; Sowmya, A., An Underwater Color Image Quality Evaluation Metric. *IEEE Transactions on Image Processing* **2015,** 24, (12), 6062-6071.
46. Feng, W.; Lu, H.; Yao, T.; Yu, Q., Drought characteristics and its elevation dependence in the Qinghai–Tibet plateau during the last half-century. *Scientific Reports* **2020,** 10, (1), 14323.
47. Zhu, L.; Kong, L.; Zhang, C., Numerical Study on Hysteretic Behaviour of Horizontal-Connection and Energy-Dissipation Structures Developed for Prefabricated Shear Walls. *Applied Sciences* **2020,** 10, (4), 1240.
48. Zhang, W., Parameter Adjustment Strategy and Experimental Development of Hydraulic System for Wave Energy Power Generation. *Symmetry* **2020,** 12, (5), 711.
49. Yang, Y.; Liu, J.; Yao, J.; Kou, J.; Li, Z.; Wu, T.; Zhang, K.; Zhang, L.; Sun, H., Adsorption behaviors of shale oil in kerogen slit by molecular simulation. *Chemical Engineering Journal* **2020,** 387, 124054.

50. Yan, J.; Pu, W.; Zhou, S.; Liu, H.; Bao, Z., Collaborative detection and power allocation framework for target tracking in multiple radar system. *Information Fusion* **2020,** 55, 173-183.
51. Wang, Y.; Yao, M.; Ma, R.; Yuan, Q.; Yang, D.; Cui, B.; Ma, C.; Liu, M.; Hu, D., Design strategy of barium titanate/polyvinylidene fluoride-based nanocomposite films for high energy storage. *Journal of Materials Chemistry A* **2020,** 8, (3), 884-917.
52. Lv, Q.; Liu, H.; Yang, D.; Liu, H., Effects of urbanization on freight transport carbon emissions in China: Common characteristics and regional disparity. *Journal of Cleaner Production* **2019,** 211, 481-489.
53. Lu, H.; Tian, P.; He, L., Evaluating the global potential of aquifer thermal energy storage and determining the potential worldwide hotspots driven by socio-economic, geo-hydrologic and climatic conditions. *Renewable and Sustainable Energy Reviews* **2019,** 112, 788-796.
54. Zhang, B.; Xu, D.; Liu, Y.; Li, F.; Cai, J.; Du, L., Multi-scale evapotranspiration of summer maize and the controlling meteorological factors in north China. *Agricultural and Forest Meteorology* **2016,** 216, 1-12.
55. Li, Z.-G.; Cheng, H.; Gu, T.-Y., Research on dynamic relationship between natural gas consumption and economic growth in China. *Structural Change and Economic Dynamics* **2019,** 49, 334-339.
56. Zhang, C.; Wang, H., Swing vibration control of suspended structures using the Active Rotary Inertia Driver system: Theoretical modeling and experimental verification. *Structural Control and Health Monitoring* **2020,** 27, (6), e2543.
57. Zhang, C.; Abedini, M.; Mehrmashhadi, J., Development of pressure-impulse models and residual capacity assessment of RC columns using high fidelity Arbitrary Lagrangian-Eulerian simulation. *Engineering Structures* **2020,** 224, 111219.
58. Yue, H.; Wang, H.; Chen, H.; Cai, K.; Jin, Y., Automatic detection of feather defects using Lie group and fuzzy Fisher criterion for shuttlecock production. *Mechanical Systems and Signal Processing* **2020,** 141, 106690.
59. Gholipour, G.; Zhang, C.; Mousavi, A. A., Numerical analysis of axially loaded RC columns subjected to the combination of impact and blast loads. *Engineering Structures* **2020,** 219, 110924.
60. Abedini, M.; Zhang, C., Performance Assessment of Concrete and Steel Material Models in LS-DYNA for Enhanced Numerical Simulation, A State of the Art Review. *Archives of Computational Methods in Engineering* **2020**.
61. Mou, B.; Zhao, F.; Qiao, Q.; Wang, L.; Li, H.; He, B.; Hao, Z., Flexural behavior of beam to column joints with or without an overlying concrete slab. *Engineering Structures* **2019,** 199, 109616.
62. Liu, J.; Wu, C.; Wu, G.; Wang, X., A novel differential search algorithm and applications for structure design. *Applied Mathematics and Computation* **2015,** 268, 246-269.
63. Abedini, M.; Mutalib, A. A.; Zhang, C.; Mehrmashhadi, J.; Raman, S. N.; Alipour, R.; Momeni, T.; Mussa, M. H., Large deflection behavior effect in reinforced concrete columns exposed to extreme dynamic loads. *Frontiers of Structural and Civil Engineering* **2020,** 14, (2), 532-553.
64. Sun, Y.; Wang, J.; Wu, J.; Shi, W.; Ji, D.; Wang, X.; Zhao, X., Constraints hindering the development of high-rise modular buildings. *Applied Sciences* **2020,** 10, (20), 7159.
65. Mou, B.; Li, X.; Bai, Y.; Wang, L., Shear behavior of panel zones in steel beam-to-column connections with unequal depth of outer annular stiffener. *Journal of Structural Engineering* **2019,** 145, (2), 04018247.
66. Wang, J.; Huang, Y.; Wang, T.; Zhang, C.; Liu, Y. h., Fuzzy finite-time stable compensation control for a building structural vibration system with actuator failures. *Applied Soft Computing* **2020,** 93, 106372.

67. Xu, M.; Li, C.; Zhang, S.; Callet, P. L., State-of-the-Art in 360° Video/Image Processing: Perception, Assessment and Compression. *IEEE Journal of Selected Topics in Signal Processing* **2020,** 14, (1), 5-26.
68. Chao, M.; Kai, C.; Zhiwei, Z., Research on tobacco foreign body detection device based on machine vision. *Transactions of the Institute of Measurement and Control* **2020,** 42, (15), 2857-2871.
69. Zenggang, X.; Zhiwen, T.; Xiaowen, C.; Xue-min, Z.; Kaibin, Z.; Conghuan, Y., Research on Image Retrieval Algorithm Based on Combination of Color and Shape Features. *Journal of Signal Processing Systems* **2019**, 1-8.
70. Xu, S.; Wang, J.; Shou, W.; Ngo, T.; Sadick, A.-M.; Wang, X., Computer Vision Techniques in Construction: A Critical Review. *Archives of Computational Methods in Engineering* **2020**.
71. Zhu, G.; Wang, S.; Sun, L.; Ge, W.; Zhang, X., Output Feedback Adaptive Dynamic Surface Sliding-Mode Control for Quadrotor UAVs with Tracking Error Constraints. *Complexity* **2020,** 2020, 8537198.
72. Xiong, Q.; Zhang, X.; Wang, W.-F.; Gu, Y., A Parallel Algorithm Framework for Feature Extraction of EEG Signals on MPI. *Computational and Mathematical Methods in Medicine* **2020,** 2020, 9812019.
73. Zhang, J.; Liu, B., A review on the recent developments of sequence-based protein feature extraction methods. *Current Bioinformatics* **2019,** 14, (3), 190-199.
74. Zhang, X.; Fan, M.; Wang, D.; Zhou, P.; Tao, D., Top-k Feature Selection Framework Using Robust 0-1 Integer Programming. *IEEE Transactions on Neural Networks and Learning Systems* **2020**, 1-15.
75. Zhao, X.; Li, D.; Yang, B.; Chen, H.; Yang, X.; Yu, C.; Liu, S., A two-stage feature selection method with its application. *Computers & Electrical Engineering* **2015,** 47, 114-125.
76. Wang, S.-J.; Chen, H.-L.; Yan, W.-J.; Chen, Y.-H.; Fu, X., Face recognition and micro-expression recognition based on discriminant tensor subspace analysis plus extreme learning machine. *Neural processing letters* **2014,** 39, (1), 25-43.
77. Xia, J.; Chen, H.; Li, Q.; Zhou, M.; Chen, L.; Cai, Z.; Fang, Y.; Zhou, H., Ultrasound-based differentiation of malignant and benign thyroid Nodules: An extreme learning machine approach. *Computer methods and programs in biomedicine* **2017,** 147, 37-49.
78. Zhang, X.; Jiang, R.; Wang, T.; Wang, J., Recursive Neural Network for Video Deblurring. *IEEE Transactions on Circuits and Systems for Video Technology* **2020**, 1-1.
79. Zhang, X.; Wang, T.; Wang, J.; Tang, G.; Zhao, L., Pyramid Channel-based Feature Attention Network for image dehazing. *Computer Vision and Image Understanding* **2020,** 197-198, 103003.
80. Chen, Z.; Wang, J.; Ma, K.; Huang, X.; Wang, T., Fuzzy adaptive two-bits-triggered control for nonlinear uncertain system with input saturation and output constraint. *International Journal of Adaptive Control and Signal Processing* **2020,** 34, (4), 543-559.
81. Huang, Z.; Zheng, H.; Guo, L.; Mo, D., Influence of the Position of Artificial Boundary on Computation Accuracy of Conjugated Infinite Element for a Finite Length Cylindrical Shell. *Acoustics Australia* **2020,** 48, (2), 287-294.
82. Tian, P.; Lu, H.; Feng, W.; Guan, Y.; Xue, Y., Large decrease in streamflow and sediment load of Qinghai–Tibetan Plateau driven by future climate change: A case study in Lhasa River Basin. *CATENA* **2020,** 187, 104340.
83. Wang, X.; Liu, Y.; Choo, K., Fault tolerant, ulti-subset aggregation scheme for smart grid. *IEEE Transactions on Industrial Informatics* **2020**.
84. Wu, C.; Wu, P.; Wang, J.; Jiang, R.; Chen, M.; Wang, X., Ontological knowledge base for concrete bridge rehabilitation project management. *Automation in Construction* **2021,** 121, 103428.
85. Hu, L.; Hong, G.; Ma, J.; Wang, X.; Chen, H., An efficient machine learning approach for diagnosis of paraquat-poisoned patients. *Computers in Biology and Medicine* **2015,** 59, 116-124.

86. Li, C.; Hou, L.; Sharma, B. Y.; Li, H.; Chen, C.; Li, Y.; Zhao, X.; Huang, H.; Cai, Z.; Chen, H., Developing a new intelligent system for the diagnosis of tuberculous pleural effusion. *Computer methods and programs in biomedicine* **2018,** 153, 211-225.
87. Zhao, X.; Zhang, X.; Cai, Z.; Tian, X.; Wang, X.; Huang, Y.; Chen, H.; Hu, L., Chaos enhanced grey wolf optimization wrapped ELM for diagnosis of paraquat-poisoned patients. *Computational Biology and Chemistry* **2019,** 78, 481-490.
88. Jalali, A.; Behrouzi, M. K.; Salari, N.; Bazrafshan, M.-R.; Rahmati, M., The effectiveness of group spiritual intervention on self-esteem and happiness among men undergoing methadone maintenance treatment. *Current Drug Research Reviews Formerly: Current Drug Abuse Reviews* **2019,** 11, (1), 67-72.
89. Salari, N.; Shohaimi, S.; Najafi, F.; Nallappan, M.; Karishnarajah, I., Application of pattern recognition tools for classifying acute coronary syndrome: an integrated medical modeling. *Theoretical Biology and Medical Modelling* **2013,** 10, (1), 57.
90. Chen, H.-L.; Wang, G.; Ma, C.; Cai, Z.-N.; Liu, W.-B.; Wang, S.-J., An efficient hybrid kernel extreme learning machine approach for early diagnosis of Parkinson′ s disease. *Neurocomputing* **2016,** 184, 131-144.
91. Mohammadi, M.; Raiegani, A. A. V.; Jalali, R.; Ghobadi, A.; Salari, N., The prevalence of retinopathy among type 2 diabetic patients in Iran: A systematic review and meta-analysis. *Reviews in Endocrine and Metabolic Disorders* **2019,** 20, (1), 79-88.
92. Liu, D.; Wang, S.; Huang, D.; Deng, G.; Zeng, F.; Chen, H., Medical image classification using spatial adjacent histogram based on adaptive local binary patterns. *Computers in biology and medicine* **2016,** 72, 185-200.
93. Chen, H.; Heidari, A. A.; Chen, H.; Wang, M.; Pan, Z.; Gandomi, A. H., Multi-population differential evolution-assisted Harris hawks optimization: Framework and case studies. *Future Generation Computer Systems* **2020,** 111, 175-198.
94. Qu, S.; Han, Y.; Wu, Z.; Raza, H., Consensus Modeling with Asymmetric Cost Based on Data-Driven Robust Optimization. *Group Decision and Negotiation* **2020**.
95. Wang, M.; Chen, H., Chaotic multi-swarm whale optimizer boosted support vector machine for medical diagnosis. *Applied Soft Computing Journal* **2020,** 88.
96. Cao, Y.; Li, Y.; Zhang, G.; Jermsittiparsert, K.; Nasseri, M., An efficient terminal voltage control for PEMFC based on an improved version of whale optimization algorithm. *Energy Reports* **2020,** 6, 530-542.
97. Zhang, Y.; Liu, R.; Wang, X.; Chen, H.; Li, C., Boosted binary Harris hawks optimizer and feature selection. *Engineering with Computers* **2020**.
98. Mi, C.; Cao, L.; Zhang, Z.; Feng, Y.; Yao, L.; Wu, Y., A port container code recognition algorithm under natural conditions. *Journal of Coastal Research* **2020,** 103, (SI), 822-829.
99. Cao, B.; Dong, W.; Lv, Z.; Gu, Y.; Singh, S.; Kumar, P., Hybrid Microgrid Many-Objective Sizing Optimization With Fuzzy Decision. *IEEE Transactions on Fuzzy Systems* **2020,** 28, (11), 2702-2710.
100. Shen, L.; Chen, H.; Yu, Z.; Kang, W.; Zhang, B.; Li, H.; Yang, B.; Liu, D., Evolving support vector machines using fruit fly optimization for medical data classification. *Knowledge-Based Systems* **2016,** 96, 61-75.
101. Wang, M.; Chen, H.; Yang, B.; Zhao, X.; Hu, L.; Cai, Z.; Huang, H.; Tong, C., Toward an optimal kernel extreme learning machine using a chaotic moth-flame optimization strategy with applications in medical diagnoses. *Neurocomputing* **2017,** 267, 69-84.
102. Xu, Y.; Chen, H.; Luo, J.; Zhang, Q.; Jiao, S.; Zhang, X., Enhanced Moth-flame optimizer with mutation strategy for global optimization. *Information Sciences* **2019,** 492, 181-203.
103. Xu, X.; Chen, H.-L., Adaptive computational chemotaxis based on field in bacterial foraging optimization. *Soft Computing* **2014,** 18, (4), 797-807.
104. Zhao, X.; Li, D.; Yang, B.; Ma, C.; Zhu, Y.; Chen, H., Feature selection based on improved ant colony optimization for online detection of foreign fiber in cotton. *Applied Soft Computing* **2014,** 24, 585-596.

105. Moayedi, H.; Tien Bui, D.; Gör, M.; Pradhan, B.; Jaafari, A., The Feasibility of Three Prediction Techniques of the Artificial Neural Network, Adaptive Neuro-Fuzzy Inference System, and Hybrid Particle Swarm Optimization for Assessing the Safety Factor of Cohesive Slopes. *ISPRS International Journal of Geo-Information* **2019,** 8, (9), 391.
106. Xi, W.; Li, G.; Moayedi, H.; Nguyen., H., A particle-based optimization of artificial neural network for earthquake-induced landslide assessment in Ludian county, China *Geomatics, Natural Hazards and Risk* **2019,** 10, (1), 1750-1771.
107. Zhou, G.; Moayedi, H.; Bahiraei, M.; Lyu, Z., Employing artificial bee colony and particle swarm techniques for optimizing a neural network in prediction of heating and cooling loads of residential buildings. *Journal of Cleaner Production* **2020,** 254.
108. Cao, B.; Fan, S.; Zhao, J.; Yang, P.; Muhammad, K.; Tanveer, M., Quantum-enhanced multiobjective large-scale optimization via parallelism. *Swarm and Evolutionary Computation* **2020,** 57, 100697.
109. Asadi, E.; Silva, M. G. d.; Antunes, C. H.; Dias, L.; Glicksman, L., Multi-objective optimization for building retrofit: A model using genetic algorithm and artificial neural network and an application. *Energy and Buildings* **2014,** 81, 444-456.
110. Budaiwi, I.; Abdou, A., HVAC system operational strategies for reduced energy consumption in buildings with intermittent occupancy: The case of mosques. *Energy Conv. Manag.* **2013,** 73, 37-50.
111. Nasruddin; Sholahudin; Satrio, P.; Mahlia, T. M. I.; Giannetti, N.; Saito, K., Optimization of HVAC system energy consumption in a building using artificial neural network and multi-objective genetic algorithm. *Sustain. Energy Technol. Assess.* **2019,** 35, 48-57.
112. Min, Y. R.; Chen, Y.; Yang, H. X., A statistical modeling approach on the performance prediction of indirect evaporative cooling energy recovery systems. *Appl. Energy* **2019,** 255, 13.
113. Roy, S. S.; Roy, R.; Balas, V. E., Estimating heating load in buildings using multivariate adaptive regression splines, extreme learning machine, a hybrid model of MARS and ELM. *Renew. Sust. Energ. Rev.* **2018,** 82, 4256-4268.
114. Liu, K.; Liu, T. Z.; Jian, P.; Lin, Y., The re-optimization strategy of multi-layer hybrid building's cooling and heating load soft sensing technology research based on temperature interval and hierarchical modeling techniques. *Sust. Cities Soc.* **2018,** 38, 42-54.
115. Kavaklioglu, K., Robust modeling of heating and cooling loads using partial least squares towards efficient residential building design. *J. Build. Eng.* **2018,** 18, 467-475.
116. Moayedi, H.; Mu'azu, M. A.; Foong, L. K., Novel Swarm-based Approach for Predicting the Cooling Load of Residential Buildings Based on Social Behavior of Elephant Herds. *Energy and Buildings* **2019,** 206, 109579.
117. Qiao, w.; Moayedi, H.; Foong, K. L., Nature-inspired hybrid techniques of IWO, DA, ES, GA, and ICA, validated through a k-fold validation process predicting monthly natural gas consumption. *Energy and Buildings* **2020,** In press.
118. Tsanas, A.; Xifara, A., Accurate quantitative estimation of energy performance of residential buildings using statistical machine learning tools. *Energy and Buildings* **2012,** 49, 560-567.
119. Guo, Z.; Moayedi, H.; Foong, L. K.; Bahiraei, M., Optimal Modification of Heating, Ventilation, and Air Conditioning System Performances in Residential Buildings Using the Integration of Metaheuristic Optimization and Neural Computing. *Energy and Buildings* **2020**, 109866.
120. Tien Bui, D.; Moayedi, H.; Anastasios, D.; Kok Foong, L., Predicting Heating and Cooling Loads in Energy-Efficient Buildings Using Two Hybrid Intelligent Models. *Applied Sciences* **2019,** 9, (17), 3543.
121. Gao, W.; Alsarraf, J.; Moayedi, H.; Shahsavar, A.; Nguyen, H., Comprehensive preference learning and feature validity for designing energy-efficient residential buildings using machine learning paradigms. *Applied Soft Computing* **2019,** 84, 105748.

122. McCulloch, W. S.; Pitts, W., A logical calculus of the ideas immanent in nervous activity. *The bulletin of mathematical biophysics* **1943,** 5, (4), 115-133.
123. Jain, A. K.; Mao, J.; Mohiuddin, K. M., Artificial neural networks: A tutorial. *Computer* **1996,** 29, (3), 31-44.
124. Simpson, S.; McCAFFERY, A. R.; HAeGELE, B. F., A behavioural analysis of phase change in the desert locust. *Biological Reviews* **1999,** 74, (4), 461-480.
125. Saremi, S.; Mirjalili, S.; Lewis, A., Grasshopper optimisation algorithm: theory and application. *Advances in Engineering Software* **2017,** 105, 30-47.
126. Mafarja, M.; Aljarah, I.; Faris, H.; Hammouri, A. I.; Ala'M, A.-Z.; Mirjalili, S., Binary grasshopper optimisation algorithm approaches for feature selection problems. *Expert Systems with Applications* **2019,** 117, 267-286.
127. Bayraktar, Z.; Komurcu, M.; Werner, D. H. In *Wind Driven Optimization (WDO): A novel nature-inspired optimization algorithm and its application to electromagnetics*, 2010 IEEE Antennas and Propagation Society International Symposium, 2010; IEEE: pp 1-4.
128. Derick, M.; Rani, C.; Rajesh, M.; Farrag, M.; Wang, Y.; Busawon, K., An improved optimization technique for estimation of solar photovoltaic parameters. *Solar Energy* **2017,** 157, 116-124.
129. Bayraktar, Z.; Komurcu, M.; Bossard, J. A.; Werner, D. H., The wind driven optimization technique and its application in electromagnetics. *IEEE transactions on antennas and propagation* **2013,** 61, (5), 2745-2757.
130. Roberts, A.; Marsh, A., ECOTECT: environmental prediction in architectural education. **2001**.
131. Chou, J.-S.; Bui, D.-K., Modeling heating and cooling loads by artificial intelligence for energy-efficient building design. *Energy and Buildings* **2014,** 82, 437-446.